PERFORMANCE ANALYSIS OF A DTC BASED 4S3P VSI- FED HIGH PERFORMANCE INDUCTION MOTOR DRIVE

by

Md. Khurshed Alam

A project submitted in partial fulfillment of the requirements for the degree of Master of Science in Electrical and Electronic Engineering

Khulna University of Engineering & Technology

Khulna 9203. Bangladesh

September, 2013

Declaration

This is to certify that the project work entitled "*Performance Analysis of a DTC Based 4S3P VSI- Fed High Performance Induction Motor Drive "* carried out by Md. Khurshed Alam in the Department of Electrical and Electronic Engineering, Khulna University of Engineering & Technology, Bangladesh. The above project work or any-part of the work has not been submitted anywhere for the award of any degree or diploma.

Signature of Supervisor	Signature of the Candidate
Dr. Md. Abdur Rafiq	Md. Khurshed Alam
Professor, Department of EEE,	
KUET, Khulna.	

Approval

This is to certify that the project work submitted by Md. Khurshed Alam entitled " *Performance Analysis of a DTC Based 4S3P VSI- Fed High Performance Induction Motor Drive "* has been approved by the Board of Examiners for the partial fulfillment of the requirements for the degree of Master of Science in Engineering in Electrical and Electronic Engineering Department, Khulna University of Engineering & Technology, Bangladesh in September 2013.

BOARD OF EXAMINERS

1. .....
Prof. Dr. Md. Abdur Rafiq — Chairman
Professor — (Supervisor)
Khulna University of Engineering & Technology

2. .....
Head, Department of EEE — Member
Khulna University of Engineering & Technology

3. .....
Prof. Dr. Md. Abdus Samad — Member
Department of Electrical and Electronic Engineering
Khulna University of Engineering & Technology

4. .....
Prof. Mr. A.N.M Enamul Kabir — Member
Department of Electrical and Electronic Engineering
Khulna University of Engineering & Technology

5. .....
Member
Professor — (External)
Department of Electrical and Electronic Engineering
University of Engineering & Technology

ACKNOWLEDGEMENTS

First and foremost, all praises for Allah who has given me all the help, guidance, and courage to finish my project work. May Allah help me to convey all what I learned for the benefit.

I am so thankful to my thesis supervisor Dr. Md. Abdur Rafiq for his continuous help and guidance throughout the project. As my project advisor, Dr. Md. Abdur Rafiq has given every possible effort to help me to achieve my goals. Working with him is an experience that I never forget in my life. I am also thankful to Professor Dr. Md. Rafiqul Islam, Mr. Md. Habibullah and Dr. Mohiuddin Ahmad for their help and suggestions.

I would also like to thank Dr. Asma Ferdowsi, my wife, the rest of my family, especially my father, brother, and sister, as well as my friends for their continued support. Also, I want to thanks Mr. Nazmul Haque, techniciann of Hardware lab for constructing the apparatus. I also appreciate the efforts and advice put on by the Hardware laboratory personnel.

The work presented in this project would not have been possible without the support of the Khulna University of Engineering & Technology Administration, under the grant of my proposal to Electrical and Electronic Engineering department. Finally, we would like to thank all whose direct and indirect support helped us completing my project in time.

ABSTRACT

More than two decades ago, Direct Torque Control (DTC) was introduced to give fast, effective and efficient dynamic response. DTC can be considered as an alternative to the field-oriented control (FOC) technique. In fact, a DTC scheme accomplishes the closed-loop control of the stator flux magnitude and the electromagnetic torque of the motor without the intermediary of any current loop or shaft sensor. To this end, the DTC scheme senses the stator currents and the dc-link voltage and processes them, together with the states of the inverter switches, to estimate the actual values of the controlled variables.

Many attempts have been carried out in the literature since the DTC was introduced in 1986, aiming to improve the performance of DTC of induction motor drives. Two of the major issues which are normally addressed in DTC drives are the variation of the switching frequency of the inverter used in the DTC drives with (i) operating conditions and (ii) the high torque ripple for using torque hysteresis comparator. To improve the performance of DTC, researchers consider different analytical approaches. The author proposed a constant switching frequency torque controller to replace the conventional hysteresis based controller. The hardware of a DTC scheme is reduced by using only one sensor of current and by inserting it in the inverter dc link.

Nowadays, researchers are working not only for better performance of the drives but also trying to reduce the cost of the drives. Conventional six switch three phase (6S3P) inverters have been widely used for AC motor drives for the last few decades. But the reduction of the number of power transistor switches from six to four reduces the cost of the inverter, decreases the switching losses and complexity of the control algorithms instead of generating six PWM signals. A cost effective four switch three phase (4S3P) inverter with almost similar performance is proposed for IM drives. The authors show a performance comparison of the 4S3P inverter fed drive with 6S3P inverter fed drive in terms of speed response and total harmonic distortion of the stator current. But overshoot and undershoot can not be eliminated in the speed response of the drive system. The proposed fuzzy logic controller based control scheme for 4S3P inverter has been fed in the interior permanent magnet synchronous motor (IPMSM) drive. Vector control of induction motor using 4S3P inverter for high performance industrial drive systems is presented in this paper. The 4S3P inverter fed IM drive is found quite acceptable considering its performance, cost reduction and other advantages. The proposed low cost control scheme is suitable for industry applications

CONTENTS

LIST OF TABLE

LIST OF FIGURES

Chapter I

1.1 Introduction

AC motors, especially induction motors are suitable for industrial drives, because of their simple and robust structure, high torque to weight ratio, higher reliability and ability to operate in hazardous environments. However, the control of induction motor is a challenging task as the rotor quantities are not accessible which are responsible for torque production. DC machines are decoupled in terms of flux and torque. Hence control is easy. If it is possible in case of induction motor to control the amplitude and space angle (between rotating stator and rotor fields), in other words to supply power from a controlled source so that the flux producing and torque producing components of stator current can be controlled independently, the motor dynamics can be compared to that of DC motor with fast transient response. Presently, introduction of micro-controllers, high switching frequency semiconductor devices, and VLSI technology has led to cost effective sophisticated control strategies.

A new area of ac motor drive has been highly developed by power electronics technology. In particular, squirrel cage induction motor drive "under the vector control of induction motor drive" is considered as one of the best ac variables controlled drives when quick response is required. The stator current is splitted into two orthogonal components, one in the direction of flux linkage, representing magnetizing current or flux component of current and other perpendicular to the flux linkage, representing the torque component of current. By varying both components independently, the induction motor can be treated as a separately excited DC motor. This concept was invented in the beginning of 1970s. The

Implementation of vector control requires information regarding the magnitude and position of the flux vector. Depending upon the method of acquisition of flux information, the vector control or field oriented control method can be termed as: direct or indirect. In the direct method the position of the flux is strictly measured with the help of sensors, or estimated from the machine terminal variables such as speed and stator current/voltage signals. The measured or estimated flux is used in the feedback loop, thus the machine parameters have minimal effect on the overall drive performance. But the measurement of flux using flux sensors necessitates special manufacturing process or modifications in the existing machines. In addition, the direct field orientation method has its inherent problem at low speed where the voltage drops due to resistances are dominant, and pure integration is difficult to achieve.

Recently, advanced control strategies for Pulse Width Modulation (PWM) inverter fed induction motor drive has been presented. Particularly, the vector control, which guarantees high dynamic and static performances like DC motor drives, has become very popular and has been developed and improved. Recent developments in the theory of vector control, fast digital processor and power devices provide the possibility of achieving high performance induction motor drive control.

Space Vector Modulation (SVM) technique is widely used in control of induction motor drive. This technique reduces the torque and flux ripple in induction motor drive and high performance is achieved. It contains space vectors to be applied according to the region where the output voltage vector is located. It has two excellent features such as maximum output voltage is greater and the number of switching is less at the same carrier frequency. High performance drive of an induction motor requires the rotor position information to control the motor which is generally detected by mechanical position sensors such as an

encoder or a resolver. The additional components such as resolver and position sensors not only increase the cost but also affect reliability of the system. Flux estimation can be applied to find the rotor position and is considered as an important task in implementing high performance motor drives.

Nowadays, researchers are working not only for better performance of the drives but also trying to reduce the cost of the drives. Conventional six switch three phase (6S3P) inverters have been widely used for AC motor drives for the last few decades. But the reduction of the number of power transistor switches from six to four reduces the cost of the inverter, decreases the switching losses and complexity of the control algorithms instead of generating six PWM signals. A cost effective four switch three phase (4S3P) inverter is proposed for IM drives. The authors show a performance comparison of the 4S3P inverter fed drive with 6S3P inverter fed drive in terms of speed response and total harmonic distortion of the stator current. But overshoot and undershoot can not be eliminated in the speed response of the drive system. The propose fuzzy logic controller based control scheme for 4S3P inverter fed interior permanent magnet synchronous motor (IPMSM) drive. Vector control of induction motor using 4S3P inverter for high performance industrial drive systems . In recent year , the performance of self-tuning Fuzzy PI controller is compared with the corresponding fuzzy logic controller and PI controller. The performance index based on speed error is assigned to provide a numerical comparison among different controllers. The Model Reference Adaptive System (MRAS) is used as a speed estimator and the motor is fed from a 4S3P inverter. The 4S3P inverter fed IM drive is found quite acceptable considering its performance, cost reduction and other advantages. The authors verified the complete scheme by simulation in a DSP environment.

Unfortunately observer or flux estimator has some inherent disadvantages, such as the influence of noise, the computational burden. This has led to a renewed interest to the field of flux estimation. Recently, AI (artificial intelligent) techniques such as expert system,fuzzy logic, and artificial neural networks (ANN) are showing much promise for intelligent adaptive control and estimation of parameters and variables of motor drives. The machine terminal voltages and currents can be sensed and processed to calculate speed, position,flux, torque, power and other feedback signals with the help of a microprocessor. The inaccuracy of estimated signals due to machine parameter variation always remains a problem. Accurate identification of machine parameters to compensate the estimation error is a challenging task. In addition, direct integration of machine voltages near zero speed to calculate the flux is another problem because of offset problem of the integrator. The flux of a machine can be conveniently estimated from the stator voltage model at higher speed range and rotor current model at low speed range. The stator flux can be estimated using ANNs for better accuracy.

1.2 Literature Review

At present induction motors are widely used for variable speed energy converting devices in industrial and domestic appliances. They are simple, rugged, inexpensive and available at all power ratings. Progress in the field of power electronics and microelectronics enables the application of induction motors for high performance drives, where traditionally only DC motors were applied [1]. Speed and torque control mechanisms are very much essential in recent electrical motor drives [2-3].
High Performance Control (HPC) of induction motors is an interesting area for research and has wide applications in lathe machines, robotics etc. The main objective of high performance controller is to obtain fast dynamic response of the drive system. It is so

designed that it becomes less sensitive to motor and controller parameter perturbations and require minimum hardware for its practical implementation. The field-oriented control (FOC) technique is widely used in high performance motion control of induction motors. Because of torque/flux decoupling, FOC achieved good dynamic response and accurate motion control as separately excited dc motors. Two types of field orientation control schemes are used for induction motor control; first one is direct and the other is indirect control methods. In the indirect control method, the major problem is the rotor time constant, which is sensitive to both the temperature and flux level variations. When the estimation of this parameter is incorrect, the slip frequency is also incorrect and flux angle is no longer appropriate for field-orientation [4]. Direct field- orientation control is sensitive to stator resistance and total leakage inductance. In direct field-orientation, if a flux regulator is employed, the parameter sensitivity is less than the indirect field-orientation control. In an induction motor under field-orientation control, the flux can be adjusted to meet control requirement than that of permanent magnet motor field-orientation [5].

With the invention of high speed power semiconductor devices 6-Switch 3-Phase (6S3P) inverters become popular for variable speed ac drives. These inverters have some disadvantages such as losses in the six switches, complexity of the control algorithms and generating six PWM logic signals [6-10]. Many researchers have been working in this area to reduce the inverter size and cost without altering the drive performances. In [6], an ac to ac converter was developed for IM with least hardware and improved power factor. A cost effective 4-Switch 3-Phase (4S3P) inverter was proposed for IM and PMSM drives in [7-8]. The inverter consists of four switches instead of six and hence improves the inverter performance. The authors also showed a performance comparison of the 4S3P inverter fed drive with 6S3P inverter fed drive in terms of speed response and total harmonic distortion of the stator current. A Fuzzy Logic based control scheme was proposed for 4S3P fed PMSM drive in [9]. A vector control scheme of IM using 4S3P inverter for high performance industrial drive systems was presented in [10]. The complete vector control scheme was verified by simulation and experimentation in a DSP environment. Therefore, 4S3P inverter is becoming better candidate of power inverters.

The control objective requires the rotor position and/or speed of the motor to follow a preselected time tagged trajectory, regardless of unknown load variation and other parameter uncertainties. The additional components such as resolver and position sensors not only increase the cost but also affect reliability of system. Flux estimation can be applied to find the rotor position and is considered as an important task in implementing high performance motor drives.

The application of ANN attracts the attention of many scientists from all over the world [11]. The reason for this trend is the many advantages which the architectures of NN have over traditional algorithmic methods. Among the advantages of ANN, the ease of training and generalization, simple architecture, possibility of approximating nonlinear functions, insensitivity to the distortion of the network, and inexact input data are worth mentioning.
The main problem of ANNs such as BP and RTRL algorithms is that the optimal procedure is easily trapped into local minimum value and the speed of convergence is very slow. To avoid this problem, non-uniform periodicity property of chaos is used in [12-13] and starts its improvement from the learning rate. In [12], the authors show that the improved algorithm is not only efficient in internet traffic prediction with higher precision and faster speed of convergence, but also somewhat escapes the network from the problem of local minima. In [13], the authors show that, if the chaotic variation learning rate (LR) is

included during training, the weight update may be accelerated in the local minimum zone. The neural networks have become well established in induction motor drive for different tasks especially for flux estimation. Since the 1990s, several investigations into the applications of neural networks in the field of electrical machines and power electronics have appeared [14]. A new form of implementation of filter is proposed for stator flux vector synthesis that uses a combination of recurrent neural network trained by Kalman filter and a polynomial neural network in [15]. Correlated real time recurrent learning (CRTRL) neural networks has been introduced in [16] that uses α- and β-axis flux Components coupling for the flux estimation rather decoupling them.

Incorporation of chaos in induction motor is recently a hot topic in research area. Researchers consider chaotic properties for different aspects to induction motor in [17-19]. A new chaotic pulse width modulation (PWM) scheme is proposed and implemented for AC motors, which functions to suppress significantly the harmonic peaks and hence the acoustic noise in [17-18]. In [19], the authors propose a new application of a chaos particle swarm optimization (PSO) algorithm for loss model-based energy efficient control of an induction machine (IM) using an optimal rotor flux reference. The flux observers based on recurrent neural network (RNN) methods are implemented in [20] in which mean square error (MSE) values of the rotor flux estimation are between 0.000087 and 0.000264. But yet now, no literature is available to the authors for chaotic learning based ANN for flux estimation of induction motor drive.

To exploit the benefits of sensor less control, the speed estimation methods must achieve robustness against model and parameter uncertainties. Parameters of particular concern in the sensor less control literature are frequency-dependent *Rr* and temperature-dependent Rs and the load torque, all of which are very effective on the accurate estimation of flux and speed. To address the parameter sensitivity problem in induction motor speed sensor less control, a variety of approaches have been proposed [21-23]. But low speed estimation is a problem there. A lyapunov-function based flux and speed observer was developed [24] which can estimate *Rs* but not *Rr*. Duran et al. [25] performed a thermal-state estimation to compensate for the parameter and hence speed deviations due to heating. All researchers mentioned above proposed sensor less controller for induction motor drive and they didn't consider the saturation effects in induction motor drive. But it is well known that consideration of saturation effect improves the dynamic characteristics of induction motor drive.

1.3 Thesis Overview

The present project is organized in the following way:

Chapter-I begins with a preliminary discussion on drive systems, inverters, field oriented control pertaining to induction motor and related controller law. This is followed by an overview of a few selected contributions to indicate, in brief, the various studies that have been made over the past three decades in the area of vector controlled induction motor. It also includes the scope of the present study. The chapter concludes the contents of the study of other chapters in brief.

Chapter-II commences with IM Model, Stationary two-axis model, Synchronously rotating two-axis model, Phase relationship, Induction motor model in term of stator current and rotor flux are discusses in this chapter.

Chapter-III presents Induction motor controllers, voltage/frequency controller, vector controller ,field acceleration controllers ,direct torque controller, principles of direct torque controller, DTC controller, 4 switch 3 phase model ,DTC schematic, Models of a neuron, real time recurrent learning algorithms, Proposed stator flux estimation methodology, proposed IM control scheme, adjusting the PI gains, flux program, coordinate transforms, hysteresis current control technique are cover here.

Chapter-IV discusses stating performance of the IM motor, speed , torque and current performance under different operating conditions, sudden change of load torque, variation of stator parameters, speed reversal, ramp speed change, sudden disturbance torque are used for the remain of the research work.

Finally chapter-V includes the overall conclusions of this research work and highlights the direction of further research.

CHAPTER II

Mathematical Model of Induction Motor Drives

2.1 Introduction

A poly-phase induction motor has a complex structure comprising of mutually coupled magnetic and electric circuits. When the stator coils are excited by balanced electrical source, flux produced in the stator core sweeps past to the rotor core. The rotor coils are shorted together at both ends with the rotor bars in a squirrel cage induction motor. The mutual flux system is common to coils both in stator and rotor and is responsible for the effective operation of the motor. The leakage flux is responsible for causing voltage drop in the coils. Due to mutual coupling between stator and rotor coils, rotor receives power by induction. There are three systems of flux that may be considered in an induction motor, viz, the stator flux, the air gap flux and the rotor flux. In a dc motor, torque is viewed as the product of field flux and armature mmf, which are mutually perpendicular to each other. Similarly, in an induction motor it can be assumed that the flux of rotor and perpendicular mmf in the stator or vice versa generates the electromagnetic torque. Other viewpoint assumes power in the rotor resistance as a measure of torque expressed in synchronous watts.

To study the performance of different control systems and drives, the motor requires to be represented by a set of differential equations in time domain. Complexity arises due to variable coupling between the physical coils of the stator and the rotor. The complexity is further enhanced due to the effect of back emf in the rotor circuit. So it is not wise to model an induction motor using the physical coils.

Based on operating conditions, there are a number of mathematical models for induction motors. Mutually perpendicular stationary and synchronously rotating fictitious coils are considered to study the transient and dynamic conditions of induction motor drives.

2.2 Induction Motor Model

In an induction motor the stampings form the core which is slotted to receive the three phase windings of the stator. The windings are fed from a three phase supply. The rotor also consists of core for carrying three phase winding bars. Mathematically, a winding can be modeled as self-inductance L and some internal resistance R. Suffices s and r are introduced to indicate stator and rotor circuits respectively. The transfer of energy from stator to rotor of an induction motor takes place entirely inductively with the help of a flux mutually linking the two. That is why mutual inductance L_m exists between the two.

It is well documented in the literature that an induction motor can adequately be modeled using a two-axis reference frame. Under the usual assumptions of sinusoidal distribution of MMFs, ignoring the effect of iron loss and saturation, etc, the induction motor can be modeled in stationary reference frame and synchronously rotating reference frame.

2.2.1 Stationary Two-Axis Model

A 3-phase induction motor has three coils in the rotor and three coils in the stator. The rotor coils are rotating with an electrical angular velocity μ_r. The three-phase winding and

their orientation are shown in Fig. 2.1. It appears that the coupling between the stator and rotor coils is a function of position of the rotor and is continuously variable. So it is not wise to model an induction motor using its physical windings. The variables of an induction motor are phases and it can be modeled by equivalent two windings in lieu of three. In this consideration, three stationary stator windings may easily be represented by two equivalent stationary windings. To avoid the complexity of variable coupling, two equivalent stationary windings are considered for rotor circuit. Fig. 2.2 shows the mutually perpendicular fictitious coils of the three-phase equivalent of induction motor. In this connection, voltages due to rotor speed are duly considered. In the mutually perpendicular frame, there is no coupling between the axes quantities, which results in a simple system. Considering the voltage drops in the stator due to resistance, self and mutual inductances, the stator circuit equations are written. In addition to these the speed voltage terms are considered for rotor circuit only. The stator and rotor circuit voltage equations of an induction motor are given in (2.1). Well judged assumptions of no saturation, sinusoidal distribution of flux and mmf and ignoring the effect of iron loss results this set of equations. The stationary axes are indicated as ~ and [26, 27]:

$$\begin{bmatrix} v_{\sim s} \\ v_{s} \\ 0 \\ 0 \end{bmatrix} = \begin{bmatrix} R_s + L_s p & 0 & L_m p & 0 \\ 0 & R_S + L_S p & 0 & L_m p \\ L_m p & L_m \mu_r & R_r + L_r p & L_r \mu_r \\ -L_m \mu_r & L_m p & -L_r \mu_r & R_r + L_r p \end{bmatrix} \begin{bmatrix} i_{\sim s} \\ i_{s} \\ i_{\sim r} \\ i_{r} \end{bmatrix} \tag{2.1}$$

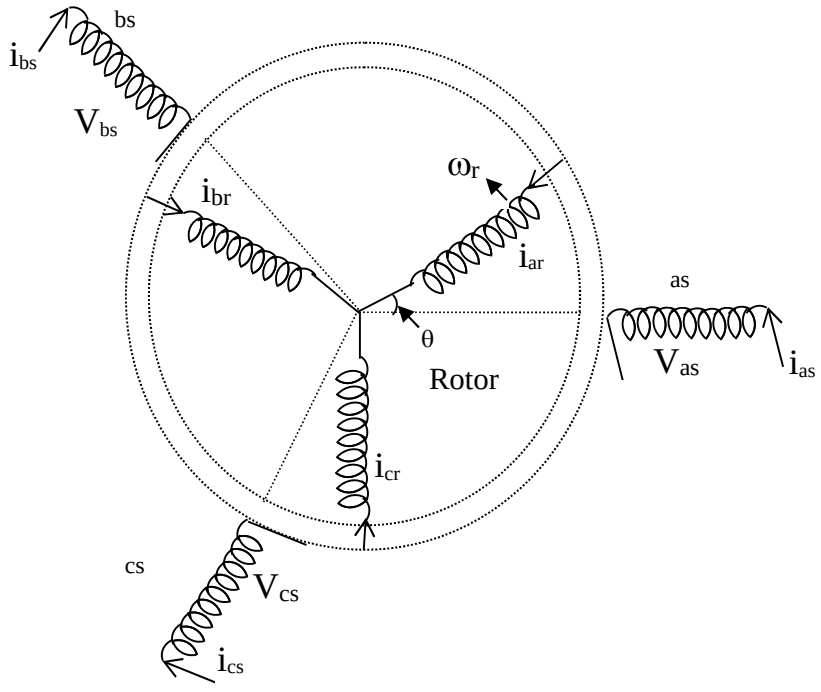

Figure 2.1 Physical Coil system of the stator and the rotor of a 3-phase induction motor.

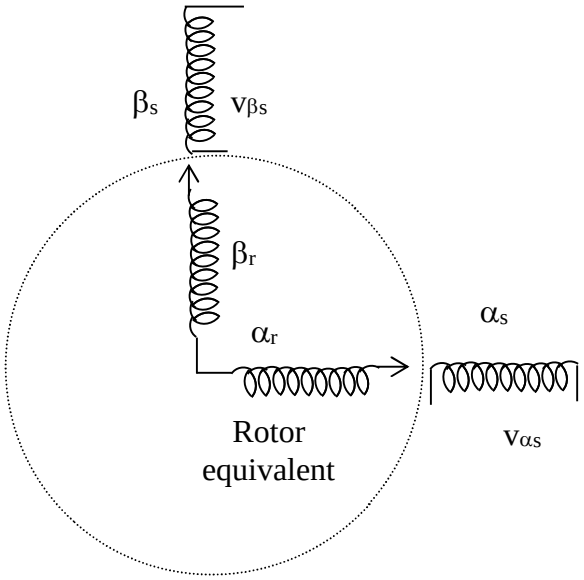

Figure 2.2 Mutually perpendicular fictitious coils of the 3-phase equivalent of induction motor.

The developed electro-magnetic torque of an induction motor of P_p -pole pairs is:

$$T_e = \frac{3}{2} P_p \left(i_{\sim r} \left[L_m i_{\ s} + L_r i_{\ r} \right] - i_{\ r} \left[L_m i_{\sim s} + L_r i_{\sim r} \right] \right) \tag{2.2}$$

In terms of stator current and stator flux the equation (2.2) can be expressed as:

$$T_e = \frac{3}{2} P_p \left(\cdot_{\sim s} i_{\ s} - \cdot_{\ s} i_{\sim s} \right) \tag{2.3}$$

where,

$$\bar{\cdot}_{\ s} = L_s \bar{i}_s + L_m \bar{i}_r \tag{2.4a}$$

$$\bar{\cdot}_{\ r} = L_r \bar{i}_r + L_m \bar{i}_s \tag{2.4b}$$

$\bar{i}_s = [i_{\sim s} \quad i_{\ s}]^T$ and $\bar{i}_r = [i_{\sim r} \quad i_{\ r}]^T$ are the stator flux, the rotor flux, the stator current and the rotor current vectors respectively.
And the torque balance equation is

$$T_e = J \frac{d\mu_m}{dt} + B\mu_m + T_L \tag{2.5}$$

Where, $\mu_m = \frac{\mu_r}{P_p}$

2.2.2 Synchronously Rotating Two-Axis Model

It is well known that the flux and mmf of an induction motor are synchronously rotating. To visualize the phenomenon of torque production and performance of the induction motor the synchronously rotating mutually perpendicular axes system is considered. This model is also suitable for current fed inverter-coupled system. According to two-axis machine

theory, when a symmetrical induction motor is described in a reference frame that rotates in synchronism with the stator mmf, all the ac phase-variable sets get transformed into equivalent dc variables. Under the usual assumptions of no hysteresis, eddy currents, space harmonics, etc., the basic system of equations of an induction motor in terms of a 2-phase model (d-q variables) in an arbitrary synchronous reference frame is given by [26]:

$$\begin{bmatrix} v_{ds} \\ v_{qs} \\ 0 \\ 0 \end{bmatrix} = \begin{bmatrix} R_s + pL_s & -\omega_e L_s & pL_m & -L_m\omega_e \\ \omega_e L_s & R_s + pL_s & L_m\omega_e & pL_m \\ pL_m & -L_m\omega_{sl} & R_r + pL_r & -L_r\omega_{sl} \\ L_m\omega_{sl} & pL_m & L_r\omega_{sl} & R_r + pL_r \end{bmatrix} \begin{bmatrix} i_{ds} \\ i_{qs} \\ i_{dr} \\ i_{qr} \end{bmatrix} \tag{2.6}$$

Fig. 2.3 shows the spatial relationship between the axes of different frames of reference viz. stator-fixed, rotor-fixed, and synchronously rotating d-q reference frames.
The developed electromagnetic torque is:

$$T_e = \frac{3}{2} P_p L_m \left(i_{qs} i_{dr} - i_{ds} i_{qr} \right) \tag{2.7}$$

Equation (2.6) and equation (2.7) can be rearranged as follows:

$$\bar{v}_s^s = R_s \bar{i}_s^s + \frac{d}{dt} \bar{\lambda}_s^s + j\omega_e \bar{\lambda}_s^s \tag{2.8a}$$

$$0 = R_r \bar{i}_r^s + \frac{d}{dt} \bar{\lambda}_r^s + j\omega_{sl} \bar{\lambda}_r^s \tag{2.8b}$$

$$T_e = \frac{3}{2} P_p \left(\lambda_{ds} i_{qs} - \lambda_{qs} i_{ds} \right) \tag{2.9}$$

Where,

$$\bar{\lambda}_s^s = L_s \bar{i}_s^s + L_m \bar{i}_r^s \tag{2.10a}$$

$$\bar{\lambda}_r^s = L_r \bar{i}_r^s + L_m \bar{i}_s^s \tag{2.10b}$$

and $\bar{v}_s^s = [v_{ds} \quad v_{qs}]^T$ is the stator voltage vector, $\bar{i}_s^s = [i_{ds} \quad i_{qs}]^T$ and $\bar{i}_r^s = [i_{dr} \quad i_{qr}]^T$ are the stator and rotor current vectors, ω_e is the speed of the synchronous reference frame, ω_{sl} is the slip speed, R_s, R_r are the stator and rotor resistances, and $\bar{\lambda}_s^s = [\lambda_{ds} \quad \lambda_{qs}]^T$ and $\bar{\lambda}_r^s = [\lambda_{dr} \quad \lambda_{qr}]^T$ are the stator and rotor flux linkage vectors respectively. The superscript "s" in the above equations denotes that the quantity is referred to the synchronous reference frame. Here, the variables $[\lambda_{ds} \quad \lambda_{qs}]$ and $[\lambda_{dr} \quad \lambda_{qr}]$ imply the flux linkages with the stator and rotor circuits along the synchronously rotating d- and q-axis respectively.
With reference to Fig. 2.4 if i_s is the magnitude of the vector current $\bar{I}_s$, the corresponding d- and q-axis currents in the synchronous reference frame are:

$$\begin{aligned} i_{ds} &= i_s g_{ds} \\ i_{qs} &= i_s g_{qs} \end{aligned} \tag{2.11}$$

Where

$g_{ds} = \cos$

$$g_{qs} = \sin^{-}$$

$$\tan^{-} = \frac{i_{qs}}{i_{ds}} \tag{2.12}$$

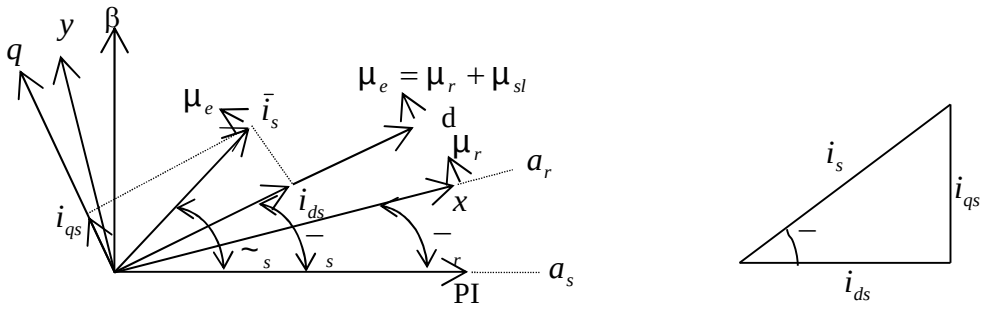

a_s - Actual stator 'a' phase axis

a_r - Actual rotor 'a' phase axis

~ – - Stator fixed reference frame

$x - y$ - Rotor fixed reference frame

$d - q$ - Synchronously rotating reference frame

$\bar{i}_s$ - Stator mmf vector

Figure 2.3 Relation between various co-ordinate systems and principle of field orientation.

2.3 Phase Relationship

1) The physical phasors and the fictitious two-axis phasors are shown in Fig. 2.4. Considering the voltages in the axes systems, the relationship among them is established as:

$$v_{\sim s} = v_a - \frac{1}{2}v_b - \frac{1}{2}v_c$$

$$v_{s} = -\frac{\sqrt{3}}{2}v_b + \frac{\sqrt{3}}{2}v_c \tag{2.13}$$

Similar relationship exists between the currents.

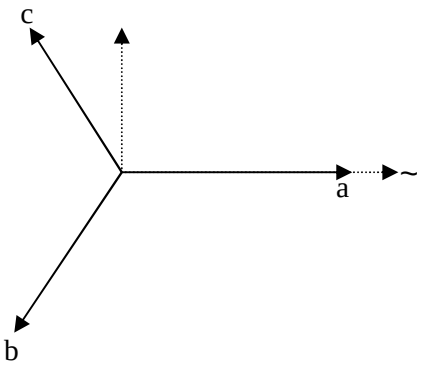

Figure 2.4 Physical 3-phase variables and their equivalent fictitious two-axis phasors.

2.4 Induction Motor Model in terms of Stator Current and Rotor Flux

In a speed controlled induction motor drive the motor is fed from a three-phase inverter. The inverter output voltage and current are controlled in a number of ways. The PWM method uses a number of positive and negative pulses per half cycle to control the magnitude and frequency of fundamental component of ac voltage. The simplest inverter generates square voltages at the output. From equation (2.1) and equation (2.2), the basic circuit equations in the stationary reference frame of induction machine can be written as:

$$\begin{bmatrix} \bar{v}_s \\ 0 \end{bmatrix} = \begin{bmatrix} (R_s + pL_s)I & pL_m I \\ pL_m I - \mu_r L_m J & (R_r + pL_r)I - L_r \mu_r J \end{bmatrix} \begin{bmatrix} \bar{i}_s \\ \bar{i}_r \end{bmatrix} \tag{2.14}$$

$$\text{and} \quad T_e = \frac{3}{2} P_p (i_{\sim r} \cdot \quad _r + i \ _r \cdot \ _{\sim r}) \tag{2.15}$$

$$\text{where,} \ \overline{\cdot}_r = L_m \bar{i}_s + L_r \bar{i}_r \tag{2.16}$$

where, $p \equiv \dfrac{d}{dt}$ is the time derivative.

The state and output equations are easily derived from equations (2.14) and (2.16) as:

$$\frac{d}{dt} \begin{bmatrix} \bar{i}_s \\ \overline{\cdot}_r \end{bmatrix} = \begin{bmatrix} A_{11} & A_{12} \\ A_{21} & A_{22} \end{bmatrix} \begin{bmatrix} \bar{i}_s \\ \overline{\cdot}_r \end{bmatrix} + \begin{bmatrix} B_1 \\ 0 \end{bmatrix} \bar{v}_s \tag{2.17}$$

$$\bar{i}_s = \begin{bmatrix} I & 0 \end{bmatrix} \begin{bmatrix} \bar{i}_s \\ \overline{\cdot}_r \end{bmatrix} \tag{2.18}$$

Where,

$$A_{11} = -\left\{ \frac{R_s}{\pm L_s} + R_r \frac{\left(1 - \pm^2\right)}{\pm L_r} \right\} I$$

$$A_{12} = \frac{L_m}{\pm L_s L_r} \left\{ \frac{R_r}{L_r} \right\} I - \mu_r J$$

$$A_{21} = \frac{L_m R_r}{L_r} I$$

$$A_{22} = -\frac{R_r}{L_r} I + \mu_r J$$

$$B_1 = \frac{1}{\pm L_s} I$$

$$I = \begin{bmatrix} 1 & 0 \\ 0 & 1 \end{bmatrix}, \ J = \begin{bmatrix} 0 & -1 \\ 1 & 0 \end{bmatrix} \tag{2.19}$$

$$\pm = 1 - \left(\frac{L_m^2}{L_s L_r} \right); \text{ leakage coefficient} \tag{2.20}$$

The state variables are the primary current $\bar{i}_s = [i_{\sim s} \quad i_{\ s}]^T$ and the rotor flux $\bar{\cdot}_r = [\cdot_{\sim r} \quad \cdot_{\ r}]^T$. The input is the primary voltage $\bar{v}_s = \left[v_{\sim s} \quad v_{\ s}\right]^T$.

2.5 Conclusion

In this chapter the induction motor model in arbitrary reference frame is discussed in detail. A dynamic model of the machine subjected to control must be known in order to understand and design high performance controlled drives. The condition to achieve field orientation control is derived.

CHAPTER III

Analysis of Direct Torque Control, ANN and Proposed Control System IM Drive

3.1 Introduction

An important factor in the worldwide industries progress during the past several decades has been the increasing sophistication of factory automation. Prior to the 1950s all such applications required the use of DC motor drives. Since Ac motors were not capable of true adjustable or smoothly varying speed since they inherently operate at synchronous speed or nearly synchronous speed with the frequency of electrical input. The inherent disadvantages of DC drives, however, have prompted continual attempt to find better solutions to the problem. To a large extent, applications that require only a gradual change in speed are now being replaced by AC drives. In general, such AC drives often feature a cost advantage over their DC counterparts and in addition offer lower maintenance, smaller motor size, and improved reliability. However, the control flexibility available with these drives is very limited. Now-a-days for high switching frequencies of modern power electronic converters with suitable control induction motor drives are superior to DC drives in industrial high-performance applications.

3.2 Induction Motor Controllers

There are many different ways for controllers to drive an induction motor. The main differences between them are the motor performance and the feasibility and cost of its real implementation. Due to the performance they are classified as:

a. Voltage/frequency controller
b. Vector controllers
c. Field acceleration controllers
d. Direct torque controllers

3.2.1 Voltage /Frequency Controllers

In spite of the fact that “voltage/frequency” (V/f) is the simplest of all controllers, it is the most widespread, used by the majority industrial applications. It is known as a scalar control and operates at magnificently constant relation maintaining between voltage and frequency. The structure is very simple and normally it is used without speed feedback. However, this controller doesn’t achieve a good accuracy in both speed and torque responses mainly due to the fact that the stator flux and the torque are not directly controlled. Even though, as long as the motor parameters are identified, the accuracy in the speed can reach within 2% (except in a very low speed) and the speed dynamic response can be approximately around 50ms[28].

3.2.2 Vector Controllers

In these types of controllers, there are control loops for controlling both the torque and flux. The most common controllers use the Park’s transformation for vector transform. Its accuracy can reach values such as within 5% regarding the speed and within 2% regarding the torque, even at stand still.

The main disadvantages of these methods are the huge computational capability requirement [29].

3.2.3 Field Acceleration Controllers

This method is based on avoiding the electromagnetic transients in the stator current, keeping the phase continuous. Therefore, the equations used can be simplified saving the vector transformation in the controllers. As it achieves some computational reduction, overcoming the main problem in vector controllers, the method becomes an important alternative for vector controllers [29].

3.3 Direct Torque Controllers

In Direct Torque Control it is possible to control the stator flux and the torque directly by selecting the appropriate inverter state. It also maintains approximately sinusoidal stator fluxes and currents. It shows high dynamic performance even at locked rotor condition. This method does not require co-ordinate transformation, voltage modulator block, as well as extra controllers such as PID for flux and torque loops. It requires minimal torque response time which is better than vector controllers. Although, some disadvantages are present in this method. It has problem during starting and it also requires flux and torque estimators, implying the consequences of parameter identification and producing inherent flux and torque ripples.

3.3.1 Principles of Direct Torque Control

The developed electromagnetic torque in three-phase induction machines can be expressed using (2.3) as follows [30]:

$$T_e = \frac{3}{2} P_p \bar{\cdot}_s \times \bar{i}_s \tag{3.1}$$

where $\bar{\cdot}_s$ is the stator flux, $\bar{i}_s$ is the stator current (both fixed to the stationary reference frame fixed to the stator) and P_p is the number of pair of poles. The above equation can be modified and expressed as follows:

$$T_e = \frac{3}{2} P_p \left|\bar{\cdot}_s\right| \cdot \left|\bar{i}_s\right| \cdot \sin(\_s - °_s) \tag{3.2}$$

where $°_s$ is the stator flux angle and $\_s$ is the stator current angle, both referred to the horizontal axis of the stationary frame fixed to the stator.

If the stator flux modulus is kept constant and the angle $\_s$ is changed quickly, then the electromagnetic torque is directly controlled.

The same conclusion can be obtained using another expression for the developed electromagnetic torque. With the help of equation (2.4), equation (3.2) can be rewritten as:

$$T_e = \frac{3}{2} P_p \frac{L_m}{L_s L_r - L_m^2} \left|\bar{\cdot}_s\right| \cdot \left|\bar{\cdot}_r\right| \cdot \sin(\_s - \_r) \tag{3.3}$$

Because the rotor time constant is larger than that of stator, the rotor flux changes slowly compared to the stator flux; in fact, the rotor flux can be assumed constant. Again, the stator flux modulus is also kept constant, and then the electromagnetic torque can be

rapidly changed and controlled by changing the angle difference ($\bar{}_s - \bar{}_r$) of the two fluxes.

3.3.2 DTC Controller

The way to impose the required stator flux is by means of choosing the most suitable Voltage Source Inverter state. If the ohmic voltage drops in the stator are neglected for simplicity, then the stator voltage impresses directly the stator flux in accordance with the following equation:

$$\frac{d\bar{\cdot}_s}{dt} = \bar{v}_s \tag{3.4}$$

It is clear from equation (3.4) that the stator flux vector $\bar{\cdot}_s$ lags the associated stator voltage vector $\bar{v}_s$ by 90 degrees.

In direct torque control, the inverter switching states are selected according to the errors of the torque and flux, which are indicated by ² and Φ respectively. Noting that:

$$² = T_e - \hat{T}_e \tag{3.5}$$

$$\Phi = \cdot_s - \hat{\cdot}_s \tag{3.6}$$

where the symbol ^ represents estimated value.

Table 3.1 shows the associated inverter switching states for two-level inverter control of the conventional direct torque approach. As shown in Table 3.1, the inverter switching states are determined by the errors of torque and flux, and the position of stator flux, which is denoted by σ_s and is given by:

$$\sigma_s = \tan^{-1}\left[\frac{\hat{\cdot}_s}{\hat{\cdot}_{\sim s}}\right] \tag{3.7}$$

The definition of states is shown in Fig. 3.1, in which the position relationship between stator voltage vector and stator flux vector is clearly indicated.

Decoupled control of the stator flux modulus and torque is achieved by acting on the radial and tangential components respectively of the stator flux–linkage space vector in its locus. These two components are directly proportional ($R_s = 0$) to the components of same voltage space vector in the same directions.

Fig. 3.1 shows the possible dynamic locus of the stator flux and the variation of stator voltage vector depending on the VSI states chosen. The possible global locus is divided into six different sectors signaled by the discontinuous line. The other two zero vectors V_0 and V_7 add to the pattern in Fig. 3.1. These vectors are associated to those inverter states with all upper half bridges switches closed, or lower switches closed, respectively. The three machine terminals are then short circuited, and the voltage vector assume zero magnitude. The existence of two zero vectors introduce an additional degree of freedom for the design of PWM strategies. These sectors of the stator flux space vector are denoted from *V0* to *V7*. Stator flux modulus error after the hysteresis block ( ) can take just two values. Torque error after the hysteresis block ( ) can take three different values. The zero voltage vectors and are selected when the torque error is within the given hysteresis limits and must remain unchanged.

Table 3.1 Look up Table for 6S3P Inverter Based Direct Torque Control

Flux error (Φ)	Torque Error (²)	$\bar{v}_s$	S_1	S_2	S_3	S_4	S_5	S_6
		— $_s$	$[0,\frac{®}{3}]$	$[\frac{®}{3},\frac{2®}{3}]$	$[\frac{2®}{3},®]$	$[®,\frac{4®}{3}]$	$[\frac{4®}{3},\frac{5®}{3}]$	$[\frac{5®}{3},2®]$
FI	TI		V_2	V_3	V_4	V_5	V_6	V_1
	T=		V_0	V_7	V_0	V_7	V_0	V_7
	TD		V_6	V_1	V_2	V_3	V_4	V_5
FD	TI		V_3	V_4	V_5	V_6	V_1	V_2
	T=		V_7	V_0	V_7	V_0	V_7	V_0
	TD		V_5	V_6	V_1	V_2	V_3	V_4

Sx: Stator flux sector
FD/FI: Flux error (Φ) decrease/increase
TI/T=/TD: Torque error (²) increase/ equal/decrease

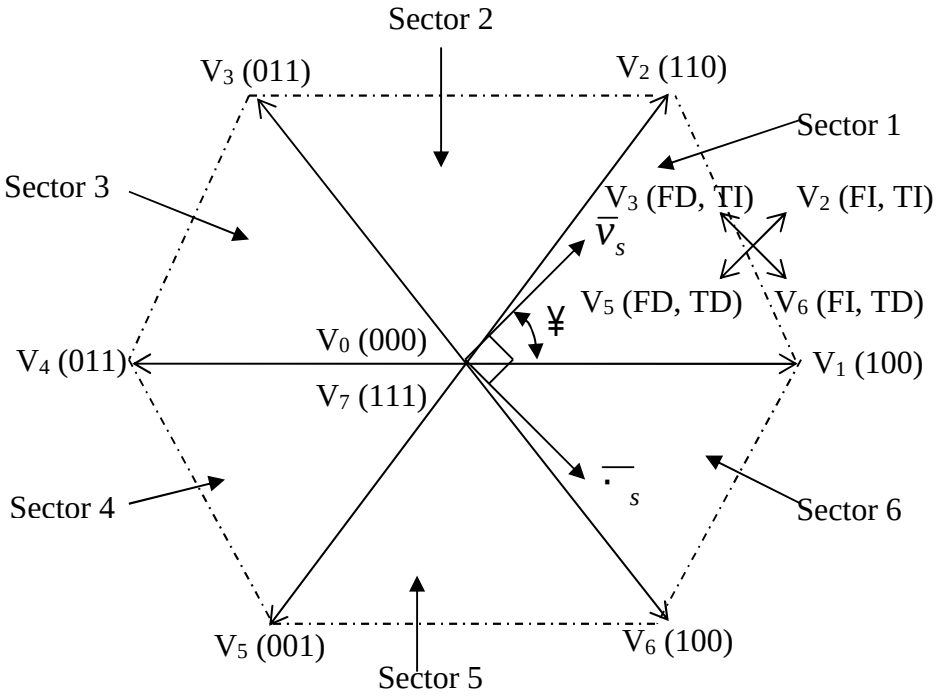

Figure 3.1 Stator flux vector locus and different possible switching voltage vectors.
FD: Flux decrease. FI: Flux Increase.
TD: Torque decrease TI: Torque Increase

3.3.3 4-Switch 3-Phase Inverter Model

In the 4-switch inverter, as shown in Fig. 3.1, a three phase voltage system is obtained by connecting the phase 'c' terminal of the stator windings directly to the centre tap of the DC link capacitors. The single phase AC supply is rectified by the front-end rectifier. The capacitors are used to level the output DC voltage. The 3-phase voltages to the IM can be expressed as follows [31]: $V_a = \frac{V_{dc}}{3}\left[4S_a - 2S_b - 1\right]$ (3.8)

$$V_b = \frac{V_{dc}}{3}\left[4S_b - 2S_a - 1\right] \quad (3.9)$$

$$V_c = \frac{2V_{dc}}{3}\left[-S_a - S_b + 1\right] \quad (3.10)$$

Where, V_{dc} is the maximum voltage across the DC link capacitors, S_a and S_b are the switching states (0 or 1) of upper switches in the legs of phases 'a' and 'b' respectively.

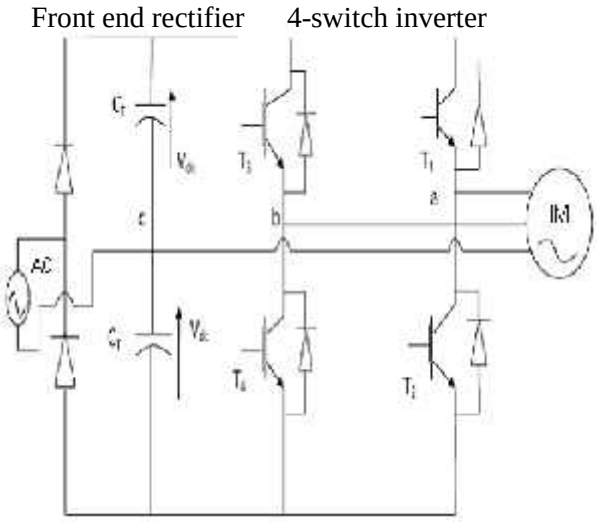

Figure 3.2 4S3P based Direct Torque Controller.

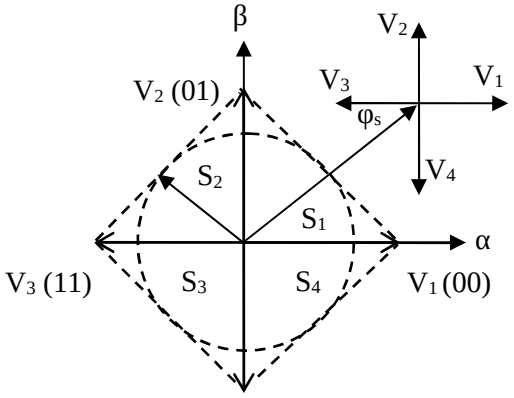

Figure 3.3 Voltage vectors of a 4-switch 3-phase inverter fed system

Table 3.2 Look up Table for 4S3P Inverter Based Direct Torque Control

¤	²	S_1	S_2	S_3	S_4
0	0	V_4	V_1	V_2	V_3
0	1	V_3	V_4	V_1	V_2
1	0	V_1	V_2	V_3	V_4
1	1	V_2	V_3	V_4	V_1

The voltage vector plane of a 4-switch inverter fed system is divided into four sectors as shown in Fig. 3.3 [32]. When the flux linkage vector stands in sector S_1, the application of voltage vector V_1 will increase the flux linkage amplitude and decrease the torque, whereas V_2 increases the flux linkage amplitude and increases the torque. Following this principle, a voltage vector switching table for the 4-switch inverter fed DTC system can be tabulated in Table 3.2.The torque and flux hysteresis comparators are two valued comparators and the output of these comparators are denoted as ² and ¤, respectively. ² or ¤ = 0 means that the actual values of these variables are above the reference and out of the hysteresis limit and ² or ¤ =1 means that the actual values of these variables are below the reference and out of the hysteresis limit.

3.3.4 DTC Schematic

Figure 3.4 shows a possible schematic of Direct Torque Control. There are two different loops corresponding to the magnitudes of the stator flux and torque. The reference values for the stator flux modulas and the torque are compared with the actual values and the resulting error values are fed into the two-level and three-level hysteresis blocks, respectively. The outputs of the stator flux error and torque error hysteresis blocks, together with the position of stator flux are used as the inputs of the look up tables (tables 3.1and 3.2). The position of the stator flux is divided into six different sectors. In accordance with Fig. 3.4, the stator flux modulus and the torque errors tend to be restricted within their respective hysteresis bands. It can be proved that the flux hysteresis band affects basically to the stator current distortion in terms of low order harmonics and the torque hysteresis band affects the switching frequency.

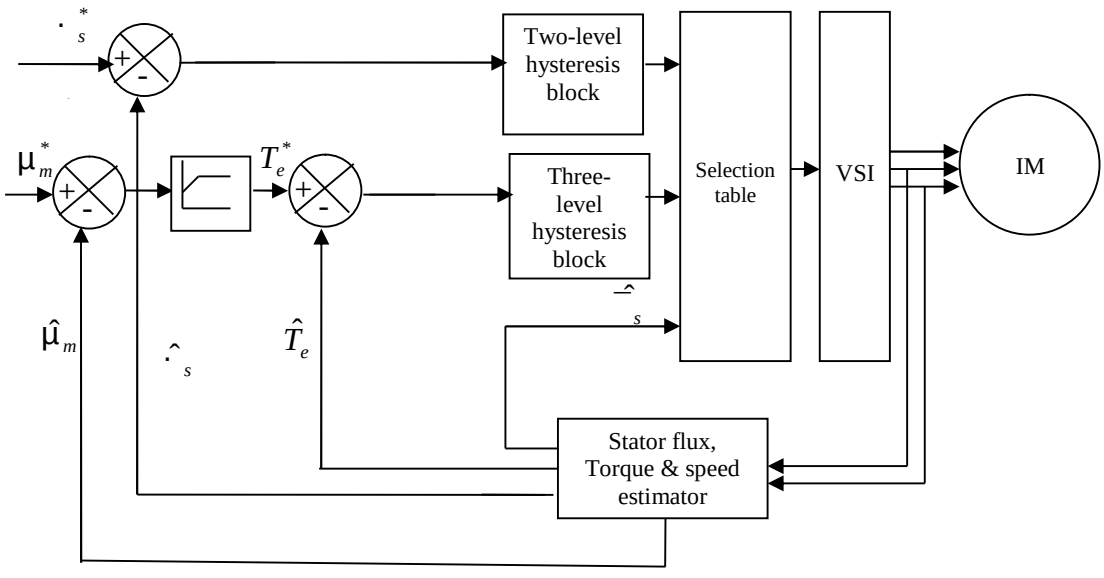

Figure 3.4 Direct Torque Controller.

3.4 Artificial Neural Network

An ANN is an information processing paradigm that is inspired by the way biological nervous systems work, such as the brain processes information [33]. The key element of this paradigm is the novel structure of the information processing system. It is composed of a large number of highly interconnected processing elements (neurons) working in unison to solve specific problems. ANN's, like human beings, learn by example. An ANN is configured for a specific application, such as pattern recognition or data classification, through a learning process. Learning in biological systems involves adjustments to the synaptic connections that exist between the neurons. This is true for ANN's as well. The use of neural networks offers the following useful properties and capabilities:

- Nonlinearity
- Input-output mapping
- Adaptivity
- Evidential response
- Contextual information
- Fault tolerance
- VLSI implementation
- Uniformity in analysis and design
- Neurobiological analogy

3.4.1 Models of a Neuron

A neuron is an information-processing unit that is fundamental to the operation of a neural network. The block diagram of Figure 3.5 shows the model of a neuron [33], which forms the basis for designing (artificial) neural networks. Here we identify three basic elements of the neuronal model:

- A set of **synapses or connecting links**, each of which is characterized by a *weight* or *strength* of its own. Specifically, a signal x_j at the input of synapse j connected to neuron k is multiplied by the synaptic weight w_{kj}. It is important to make a note of the manner in which the subscripts of the synaptic weight w_{kj} are written. The first subscript refers to the neuron in question and the second subscript refers to the input end of the synapse to which the weight refers. Unlike a synapse in the brain, the synaptic weight of an artificial neuron may lie in a range that includes negative as well as positive values.
- An **adder** for summing the input signals, weighted by the respective synapses of

the neuron; the operations described here constitutes a linear combiner.

- An activation function for limiting the amplitude of the output of a neuron. The activation function is also referred to as a squashing function in that it squashes (limits) the permissible amplitude range of the output signal to some finite value.

The neuronal model of Fig. 3.5 also includes an externally applied *bias*, denoted by b_k. that has the effect of increasing or lowering the net input of the activation function, depending on whether it is positive or negative, respectively.

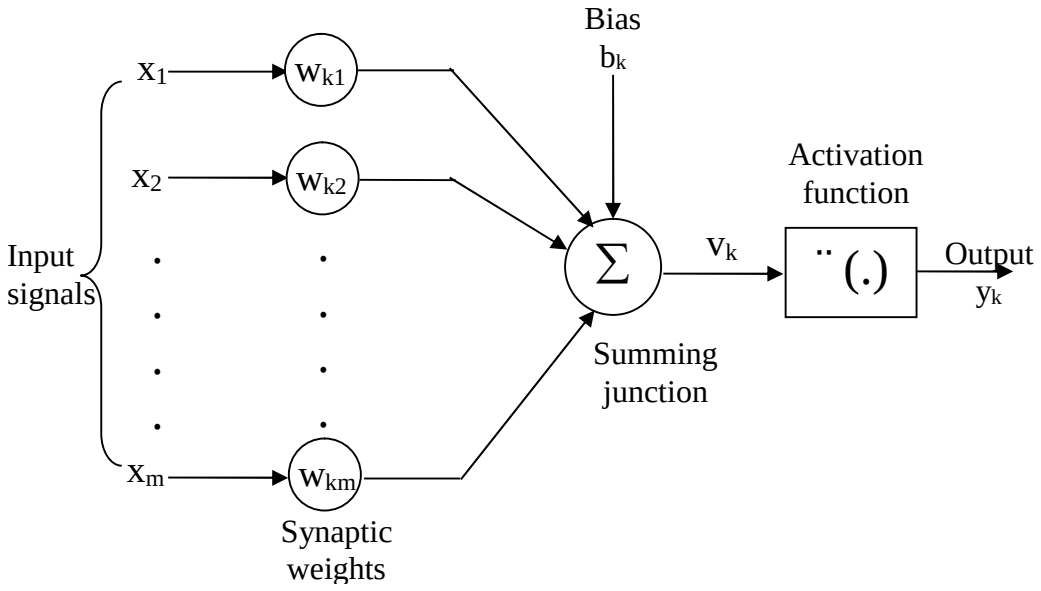

Figure 3.5 Nonlinear model of a neuron

In mathematical terms; a neuron *k* is written by the following pair of equations:

$$u_k = \sum_{j=1}^{m} w_{kj} x_j \tag{3.11}$$

and

$$y_k = \varphi(u_k + b_k) \tag{3.12}$$

where, $x_1, x_2, \ldots\ldots x_m$ are the input signals, $w_{k1}, w_{k2}, \ldots\ldots w_{km}$ are the synaptic weights of neuron k, u_k is the linear combiner output due to the input signals, b_k *is* the bias, φ(.) is the activation function and y_k the output signal of the neuron.

The use of bias b_k has the effect of applying an affine transformation to the output u_k of the linear combiner in the model of Figure 3.5, as shown by:

$$v_k = u_k + b_k \tag{3.13}$$

In particular, depending on whether the bias b_k is positive or negative, the relationship

between the induced local field or activation potential v_k of neuron k and the linear combiner output u_k *is* modified in the manner will be illustrated later*;* hereafter the term "induced local field" is used . It can be noted that as a result of this affine transformation, the graph of v_k versus u_k no longer passes through the origin.

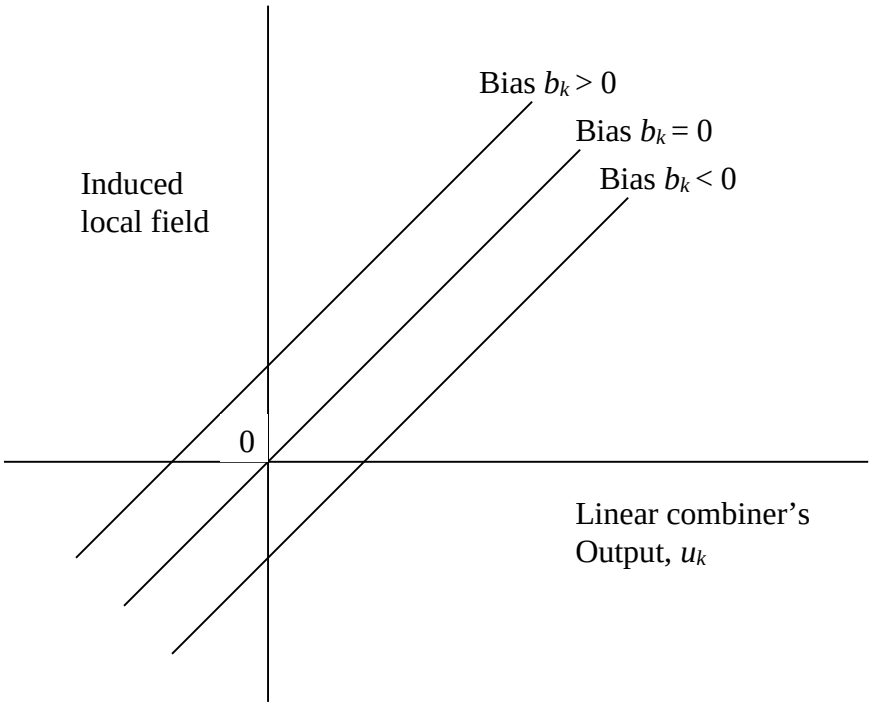

Figure 3.6 Affine transformations produced by the presence of a bias;

where $v_k = b_k$ at $u_k = 0$

The bias b_k is an external parameter of artificial neuron k. We may account for its presence as in (3.12). Equivalently, we may formulate the combination of (3.11) to (3.13) as follows:

$$v_k = \sum_{j=0}^{m} w_{kj} x_j \qquad (3.14)$$

and $y_k = \ddot{} (v_k)$ (3.15)

In Equation (3.14) we have added a new synapse. Its input is:

$X_0 = +1$ (3.16)

and its weight is:

$w_{k0} = b$ (3.17)

We may therefore, reformulate the model of neuron k as in Fig. 3.7. In this figure, the effect of the bias is accounted for by doing any two view points:

(1) Adding a new input signal fixed at +1, and

(2) Adding a new synaptic weight equal to the bias b_k.

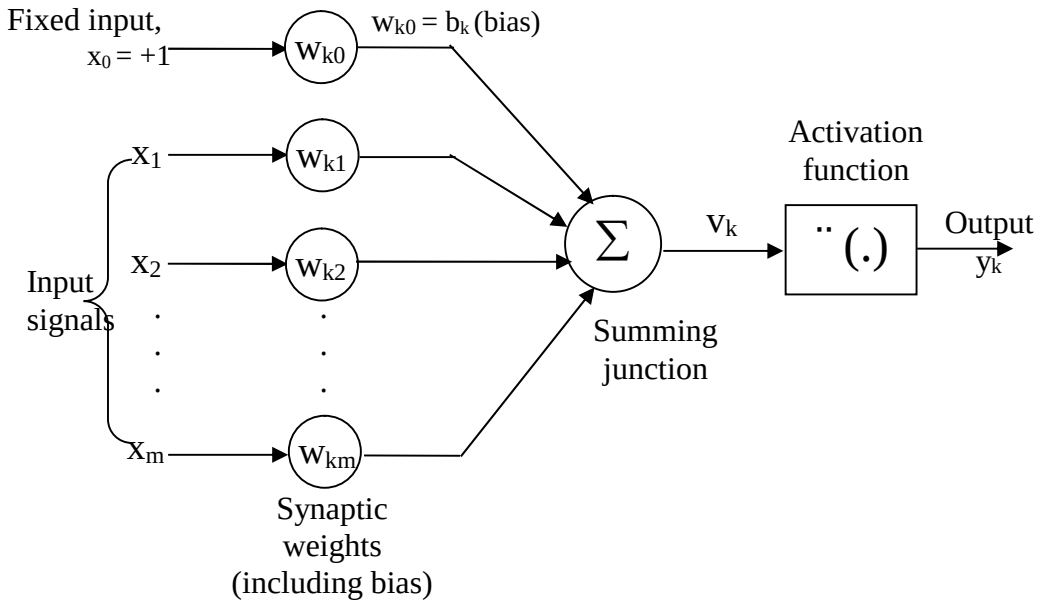

Figure 3.7 Another nonlinear model of a neuron

Although the models of Figs. 3.15 and 3.17 are different in appearance, they are mathematically equivalent.

3.4.2 Real Time Recurrent Learning Algorithms

The property that is of primary significance for a neutral network is the ability of the network to learn from environment, and to improve its performance through learning. A neural network learns from its environment through an interactive process of adjustments applied to its synaptic weights and bias levels. Ideally, the network becomes more knowledgeable about its environment after every iteration of learning process. The definition of learning in the context of neural network [33]. “Learning is a process by which the free parameters of a neural network are adapted through a process of simulation by the environment in which the network is embedded. The type of learning is determined by the manner in which the change of parameters takes place.

The RTRL algorithm derives its name from the fact that adjustments are made to the synaptic weights of a fully connected recurrent network in real time. Fig. 3.8 shows the layout of such a recurrent network [33].

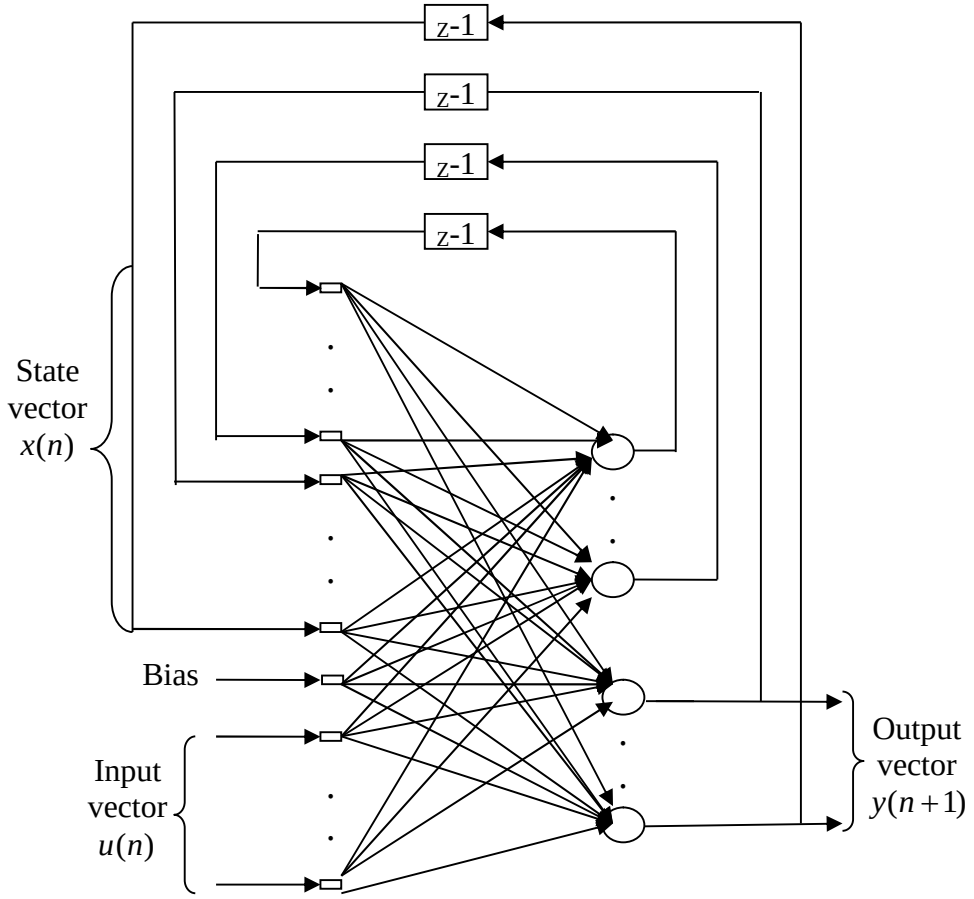

Figure 3.8 Fully connected real time recurrent network

In Mathematical terms, the dynamical behavior of any noise free system can be described by the following pair of nonlinear equations:

$$x(n+1) = \ddot{} (W_a x(n) + W_b u(n)) \qquad (3.18)$$

$$Y(n) = Cx(n) \qquad (3.19)$$

where, $x(n)$ is the q-by-1 nonlinear state matrix, $u(n)$ is the m-by-1 input matrix, $Y(n)$ is the p-by-1 corresponding output matrix, W_a is the q-by-q matrix , W_b is the q-by-(m+1) matrix and C is the p-by-q matrix.

The process equation (3.18) is reproduced here in the following expanded form:

$$x(n+1)=\begin{bmatrix} \ddot{}(w_1^T\P(n)) \\ . \\ . \\ \ddot{}(w_j^T\P(n)) \\ . \\ . \\ \ddot{}(w_q^T\P(n)) \end{bmatrix} \tag{3.20}$$

It is assumed that all the neurons have a common activation function $\ddot{}(.)$. The (q+m+1)-by-1 vector w_j is the synaptic weight vector of neuron *j* in the recurrent network, that is:

$$w_j=\begin{bmatrix} w_{a,j} \\ w_{b,j} \end{bmatrix}, j=1,2\ldots..,q \tag{3.21}$$

where $w_{a,j}$ and $w_{b,j}$ are the *jth* columns of the transposed weight matrices W_a^T and W_b^T respectively. The (q+m+1)-by-1 vector:

$$\P(n)=\begin{bmatrix} x(n) \\ u(n) \end{bmatrix} \tag{3.22}$$

The last element of $u(n)$ is +1 and, in a corresponding way, the first element of $w_{b,j}$ is equal to the bias b_j applied to neuron *j*.

The q-by- (q+m+1) partial derivative matrix of the state vector *x(n)* with respect to the weight vector w_j :

$$\Lambda_j(n)=\frac{\partial x(n)}{\partial w_j(n-1)} \quad , j=1,2,\ldots.,q \tag{3.23}$$

$U_j(n)$ is a *q*-by-(*q* +m + 1) matrix whose rows are all zero, except for the *jth* row that is equal to the transpose of vector $\P^T(n)$:

$$U_j(k)=\begin{bmatrix} 0^T \\ \P^T(n) \\ 0^T \end{bmatrix} \leftarrow jth \quad row \quad j=1,2,.....,q \tag{3.24}$$

$\ddot{}(n)$ is a *q-by-q* diagonal matrix whose *kth* diagonal element is the partial derivative of the activation function with respect to its argument, evaluated at $w_j^T\P(n)$:

$$\ddot{}(n)=diag\ [\ddot{}'(W_1^T\P(n)),\ddot{}'(W_2^T\P(n)),.....\ddot{}'(W_q^T\P(n))] \tag{3.25}$$

With these definitions, the following recursive equation Λ_j for the neuron *j* can be

obtained by differentiating (3.33) with respect to w_j and using the chain rule of calculus:

$$\Lambda_j(n+1) = \ddot{}(n)[W_a(n)\Lambda_j(n) + U_j(n)] \ , j=1,2,\ldots,q \quad (3.26)$$

The objective of the learning process is to minimize a cost function obtained by the instantaneous sum of squared errors at time *k*, which is defined in terms of *e(n)* by

$$, (n) = \frac{1}{2} e^T(n)e(n) \quad (3.27)$$

where the *p*-by-1 error vector *e(n)* is defined by using the measurement equation

$$e(n) = \tilde{y}(n) - y(n) \quad (3.28)$$

where $\tilde{y}(n)$ denotes the desired output vector.

The adjustment for the weight vector of the *jth* neuron, ΔW_j, is:

$$\Delta W_j = -\frac{\partial , (n)}{\partial W_i(n)} = C\Lambda_i(n)e(n), \quad j = 1,2,3,\ldots..,q \quad (3.29)$$

3.4.3. Input Variable Selection Methods for Artificial Neural Networks

The development of an ANN provides the non-linear transfer function
$Y = F(X) + \_$, (1)
where the model output *Y* is some variable of interest, *X* is a *k*-dimensional input vector, whose component variables are denoted by *Xi*($i = 1, \ldots, k$), and _ is some small random noise
Dynamic processes will require the development of an ANN to provide a time-series model
of the general form
$Y(t + k) = F(Y(t), \ldots, Y(t - p), X(t), \ldots, X(t - p)) + \_(t)$. (2)
Here, the output variable is predicted at some future time $t + k$, as a function of past values of both input *X* and output *Y*.

3.4.4 Proposed Stator Flux Estimation Methodology

The effectiveness of the proposed flux estimator along α-β axes needs to be verified before implementing it in the drive system. The weights of the RNN are obtained by training the neural network by CRTRL algorithm and are provided in Appendix. Real time flux components calculated from exact values of motor variables are computed and compared with the estimated flux components. Figs. 3.9 and 3.10 give a component between the actual and estimated values of α-β axes stator fluxes and rotor angle for the 4S3P and 6S3P inverter fed drive when the motor runs at 1500 rpm. A complete matching of the variables is indicated in the figures.

Clearly, the proposed RNN estimator can be used to accurately estimate stator flux components and rotor angle at both high- and low- speeds. Improvements of the performance of the drive systems are given at the finishing part of the chapter

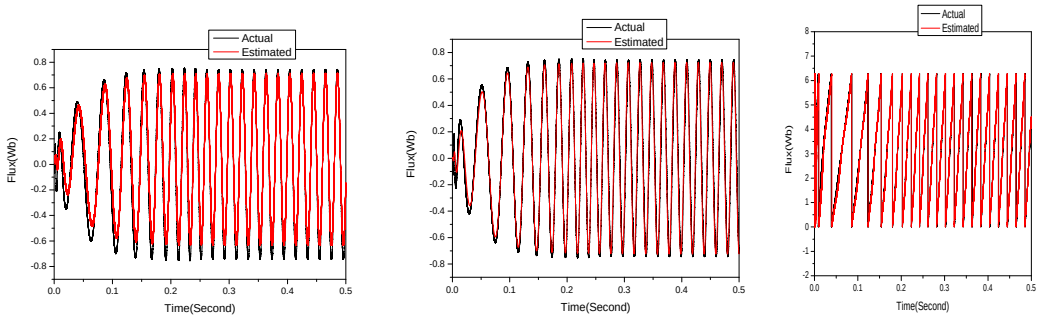

(a) (b) (c)

Fig. 3.9 Actual and estimated responses of (a) α-axis stator flux, (b) β- axis stator flux, and (c) Rotor angle for the 6S3P inverter fed IM drive transient and steady- state conditions.

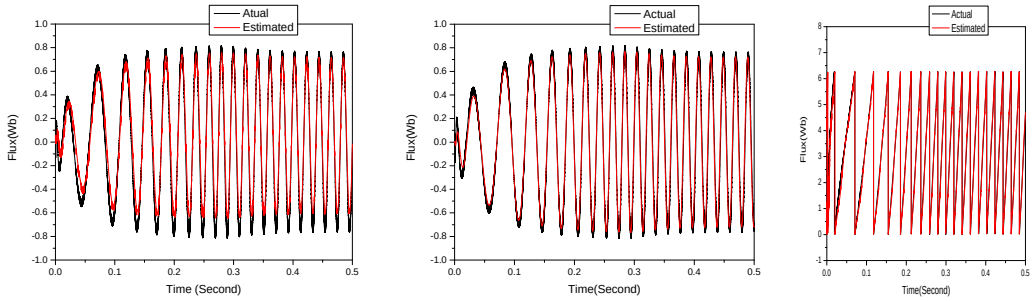

(a) (b) (c)

Fig. 3.10 Actual and estimated responses of (a) α-axis stator flux, (b) β- axis stator flux, and (c) Rotor angle for the 4S3P inverter fed IM drive under transient and steady- state

3.5 Proposed IM Control Scheme

The block diagram of a direct torque controlled IM drive system with the 4S3P inverter is shown in Fig. 3.11.

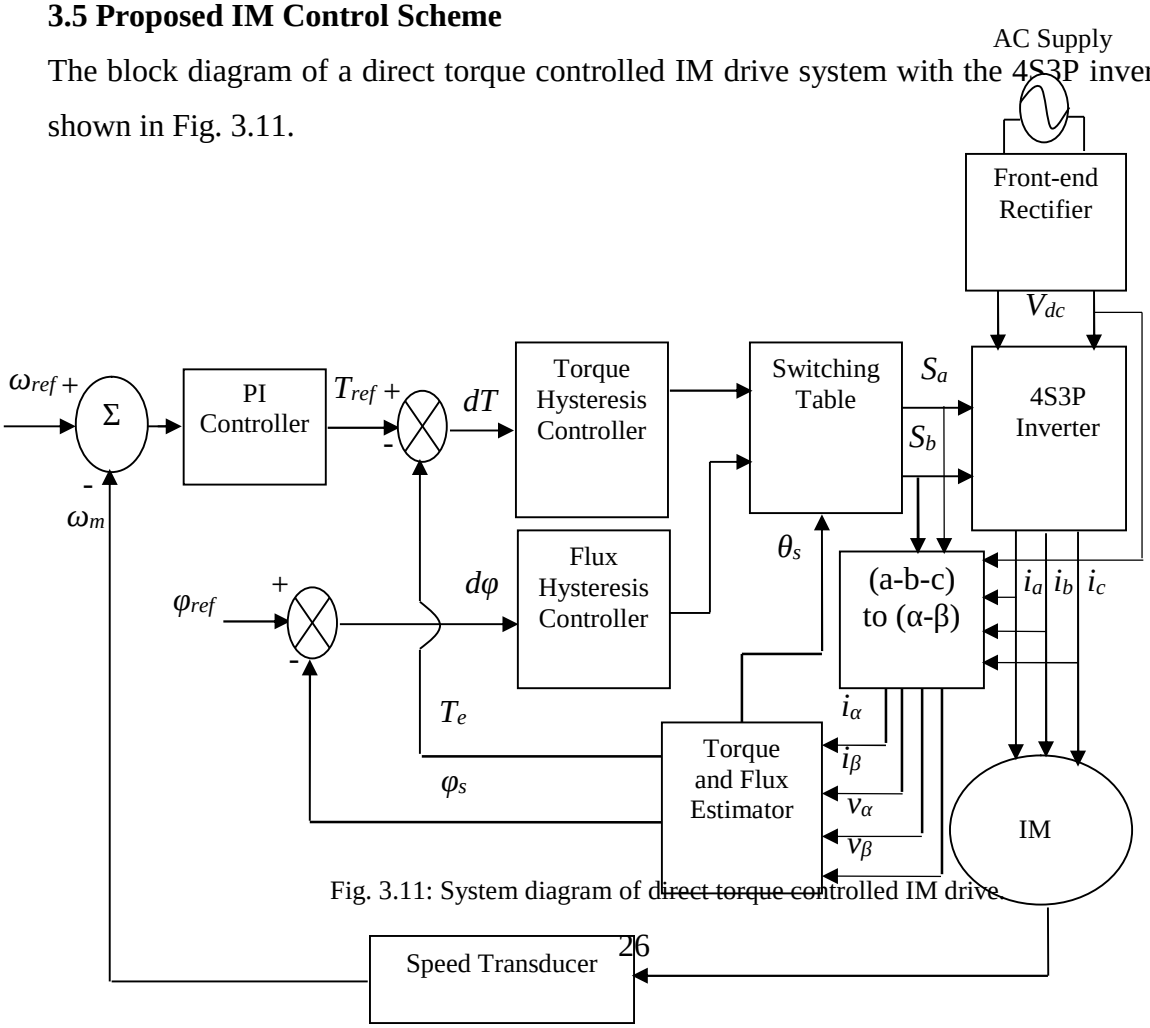

Fig. 3.11: System diagram of direct torque controlled IM drive.

The basic principle of DTC is to directly select stator voltage vectors according to the differences between the reference and actual torque and stator flux linkage. The stator flux linkage is calculated by integrating of difference between the input voltage and the voltage drop across the stator resistance. The reference torque is generated using speed error after processing through Proportional-Integral (PI) controller. The rotor angle required for vector rotation is obtained from RNN based flux and position estimator. Two independent hysteresis controllers with a suitable hysteresis band are used to command the motor currents to follow the reference currents. The hysteresis controllers also generate four switching signals which fires the power semiconductor devices of the three phase inverter to produce the actual voltage of the motor. The three phase currents are transformed into α- and β-axis components through Clarke's transformation. A speed transducer is used to measure the speed of the IM accurately.

3.5.1 **Adjusting the PI Gains**

When tuning a PI controller for first time, the I gain is set to zero. Then the P gain is increased until the system responds well to set point changes without excessive overshoot or oscillations. Using lower values of P gain will 'loosely' control the system, while higher values will give 'tighter' control. At this point, the system will probably not converge to the set point. After selecting a reasonable value of P gain, the I gain is increased slowly to force the system error to zero. Only a small amount of I gain is required in most systems. The effect of I gain, if large enough, can overcome the action of the P term, slow the overall control response and cause the system to oscillate around the set point. If oscillation occurs, reducing the I gain and increasing the P gain will usually solve the problem. There is a single PI control loop in this application. The selection of suitable values for gain constants is carried out for different combination of K_p and K_i after having their initial guesses following the ideas in [36].

3.5.2 Flux Program

In constant- torque region the torque can be controlled by i_t whereas stator flux (λ_s) can be maintained at a value determined by the flux program. The proposed control system incorporates a flux control loop where the stator flux command (λ^*_s) is generated through the flux program. The flux loop then generates magnetizing component of the stator current (i^*_m) and helps maintaining the desired λ_s irrespective of parameter variation effect.

3.5.3 Coordinate Transforms

3.5.3.1 Vector Rotator

The first coordinate transform, called the vector rotator, moves a two axis, two dimensional coordinate system, referenced to the stator, onto a three axis system, keeping the same reference. In this application, the command i_m^*
and i^*_t signals are processed through vector rotator to generate the three phase current commands for the hysteresis current controller. The stationary axes a-,b-,c-, their two

phase equivalents α-, β-, and the rotating axes of IM .The reference currents are formulated as follows

$i^*_a = i^*_m \cos\theta - i^*_t \sin\theta$

$i^*_b = i^*_m \cos(\theta\text{-}120^o) -- i^*_t \sin(\theta\text{-}120°)$

$i^*_c = i^*_m \cos(\theta + 120^o) - i^*_t \sin(\theta + 120°)$

3.5.3.2 Clarke Transform

The Clarke transform converts the stationary 3-axes (a-, b-, c-) quatities to stationary 2-axes (α-, β-) quantities by the following equations:

$$i_{as} = i_a - \frac{1}{2} i_b - \frac{1}{2} i_c$$

$$i_{\beta s} = \frac{\sqrt{3}}{2} (i_b - i_c)$$

3.5.4 Hysteresis Current Control Technique

The main task of the current is to force the current vector in the three phase load according to a reference trajectory. The scheme compares the phase currents with the desired values within the Hysteresis Band (HB) to take decision on switching of inverter transistor.

The switching logics are formulated as given below:

If $i_a < (i^*_a\text{-HB})$ T_1 on and T_2 off

If $i_a > (i^*_a\text{-HB})$ T_1 off and T_2 on

If $i_b < (i^*_b\text{-HB})$ T_3 on and T_4 off

If $i_b > (i^*_b\text{-HB})$ T_3 off and T_4 on

3.4 Conclusion

Direct torque control is a promising method. It requires the accurate estimation of rotor flux position and magnitude. Three methods are used in the study of DTC IM drive of which the integration and CRTRL methods work with better performance than the direct flux calculation method. If the performances of the former two are compared for normal and parameter deviation conditions the CRTRL method shows better performance with respect to flux angle error and torque pulsations than the integration method. This actually justifies the effectiveness of the proposed method in the induction motor control. Speed sensorless drives can be designed for DTC. In this chapter an idea concerning positions sensorless has been presented. The aim of this research was to find a position estimation scheme for the IM that is capable of working under all operating conditions, i.e. from zero to high speed and zero to full load. Therefore, a ANN based stator flux and rotor position estimator is proposed. Beside this, the application of PI controller and hysteresis current controller in the vector control of the IM drive is described briefly.

CHAPTER IV

Simulations Results and Discussions

4.1 Introduction

This chapter deals with the simulation results of the IM drive system. A simulation study is conducted in order to test the performance of the drive system. The system under consideration is simulated in C++ environment. The machine model is considered in d-q axes frame. The state space equations are solves. The sampling time for simulating the system is 5μs. Reference phase currents are generated from the torque and magnetizing currents i_t^* and i_m^*. The phase voltages V_a, V_b and V_c resulting from the hysteresis currents controller are transformed into d- and q- axis quantities V_d and V_q . Currents obtained from simulation model are transferred to get the actual phase currents. The rating and motor parameters used in this simulation. The simulation results for different operating conditions are listed in the subsequent sections.

4.2 Starting Performance of the IM Drive

The motor was started with a command speed of 1500 rpm and load torque of 1.0 N.m from standstill condition. At t=0.45 second the motor reaches to the command speed. Fig. 4.1 show the stator voltages supplied to the motor by the 6S3P inverter. In case of 4S3P inverter the a-phase and b-phase voltages have almost similar characteristics but the c-phase voltage is different in nature. Therefore, the 3- phase voltages produced by the 4S3P inverter are in unbalanced condition.

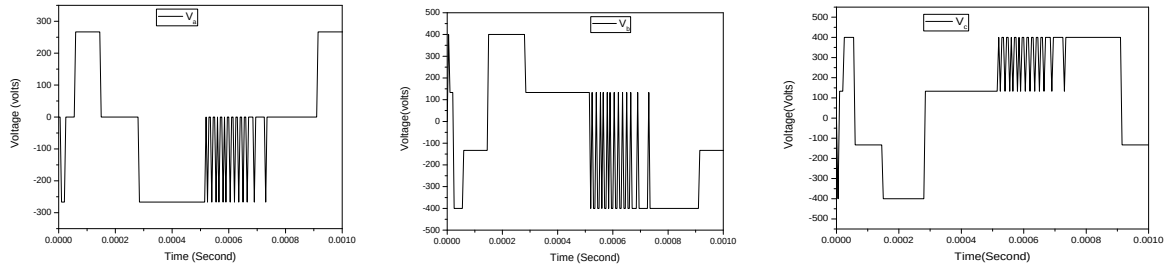

(a) (b) (c)

Figure 4.1 Stator phase voltage for the 6S3P inverted fed IM: (a) V_a, (b) V_b (c) V_c

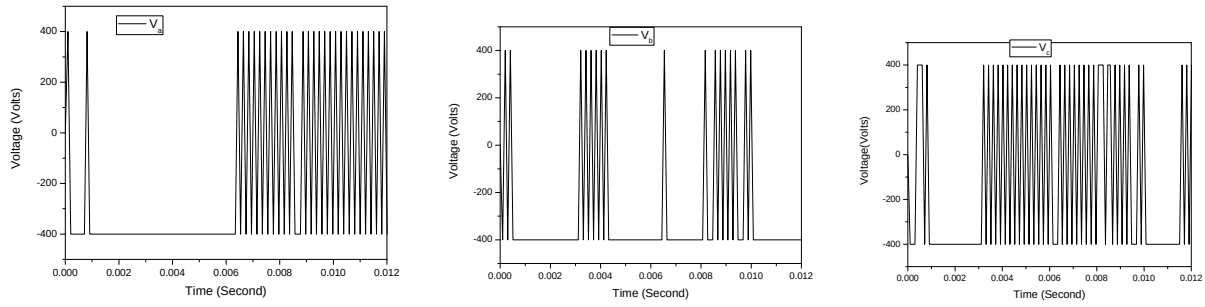

(a) (b) (c)

Figure 4.2 Stator phase voltage for the 4S3P inverted fed IM: (a) V_a, (b) V_b (c) V_c

4.3 **Speed, Torque and Current**

The motor was started with a command speed of 1500 rpm and load torque of 0 to 1 N-m from standstill condition. The 6S3P curve is shown Fig.4.3:

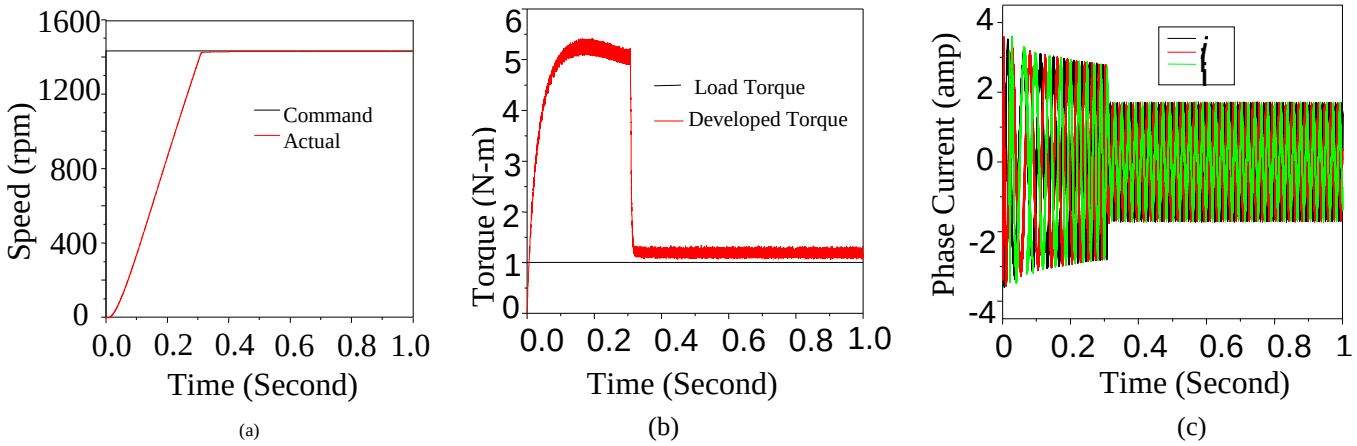

(a) (b) (c)

Figure 4.3 Speed,Torque and Current for the 6S3P inverted fed IM.

By Applying 4S3P

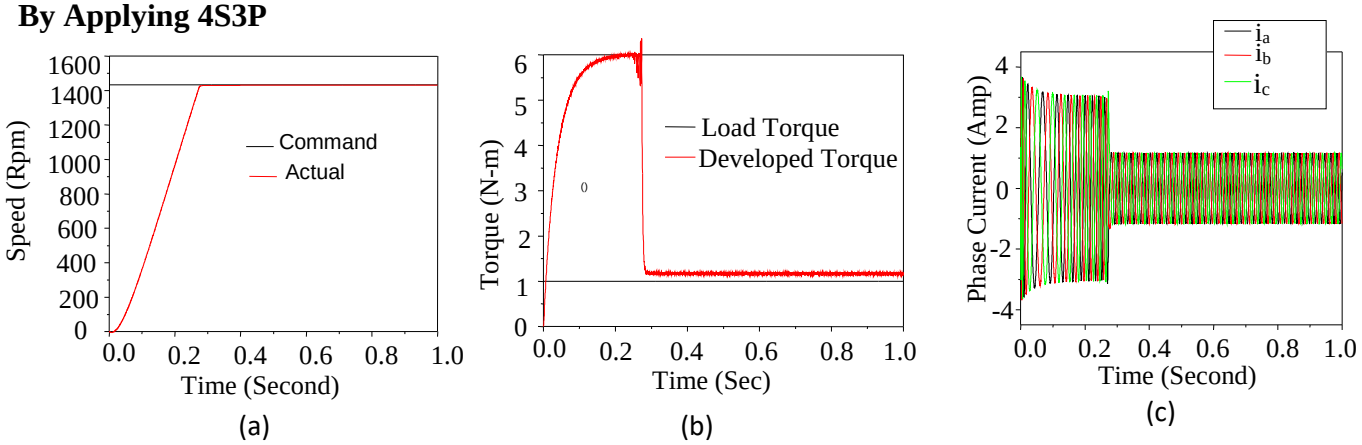

(a) (b) (c)

Figure 4.4 Speed,Torque and Current for the 4S3P inverted fed IM.

4.4 Performance under Different Operating Conditions

The performance of the IM drive under different operating conditions is also investigated in order to verify the robustness of the proposed control scheme. The corresponding responses and their descriptions are given in the following sub- sections:

4.4.1 Sudden Change of Load Torque

Initially the motor was stared from standstill with load torque 1 N.m. The estimated rotor angle and the speed responses for change of load torque in 6S3P are given in Figs. 4.5(a) and (b).The

speed response curve reached to the command speed at t=0.6sec. Sudden change of load torque does not affect the position estimation and causes a negligible oscillation in speed. Figs 4.5(c) and (d) show the corresponding torque and motor currents. The motor currents increase after 1.0 second due to the increase of load torque.

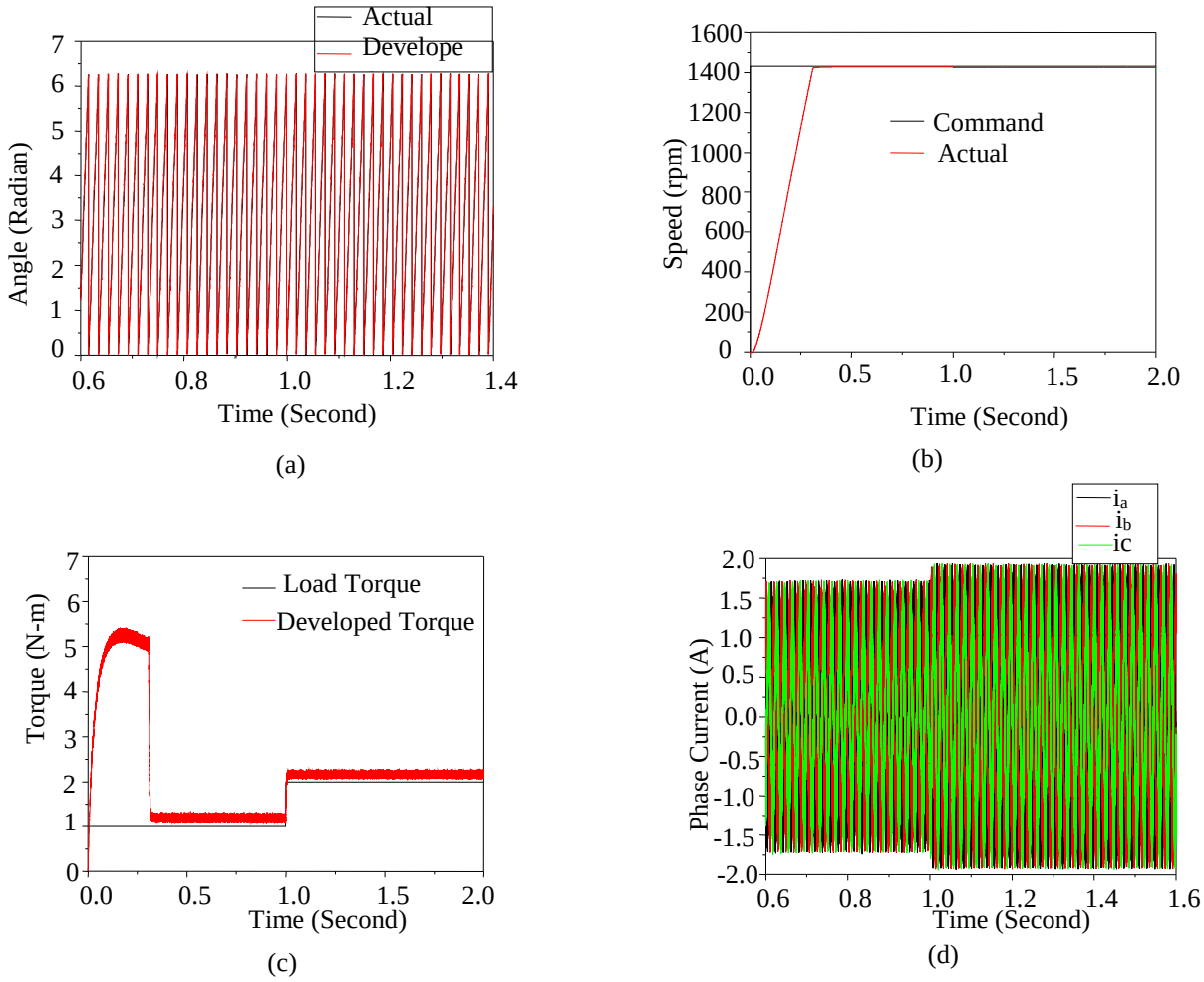

Figure 4.5 (a) Estimated rotor angle, (b) Speed, (c) Developed electromagnetic torque, and (d) Three phase currents for the proposed IM drive for change of load torque.

By applying 4S3P,

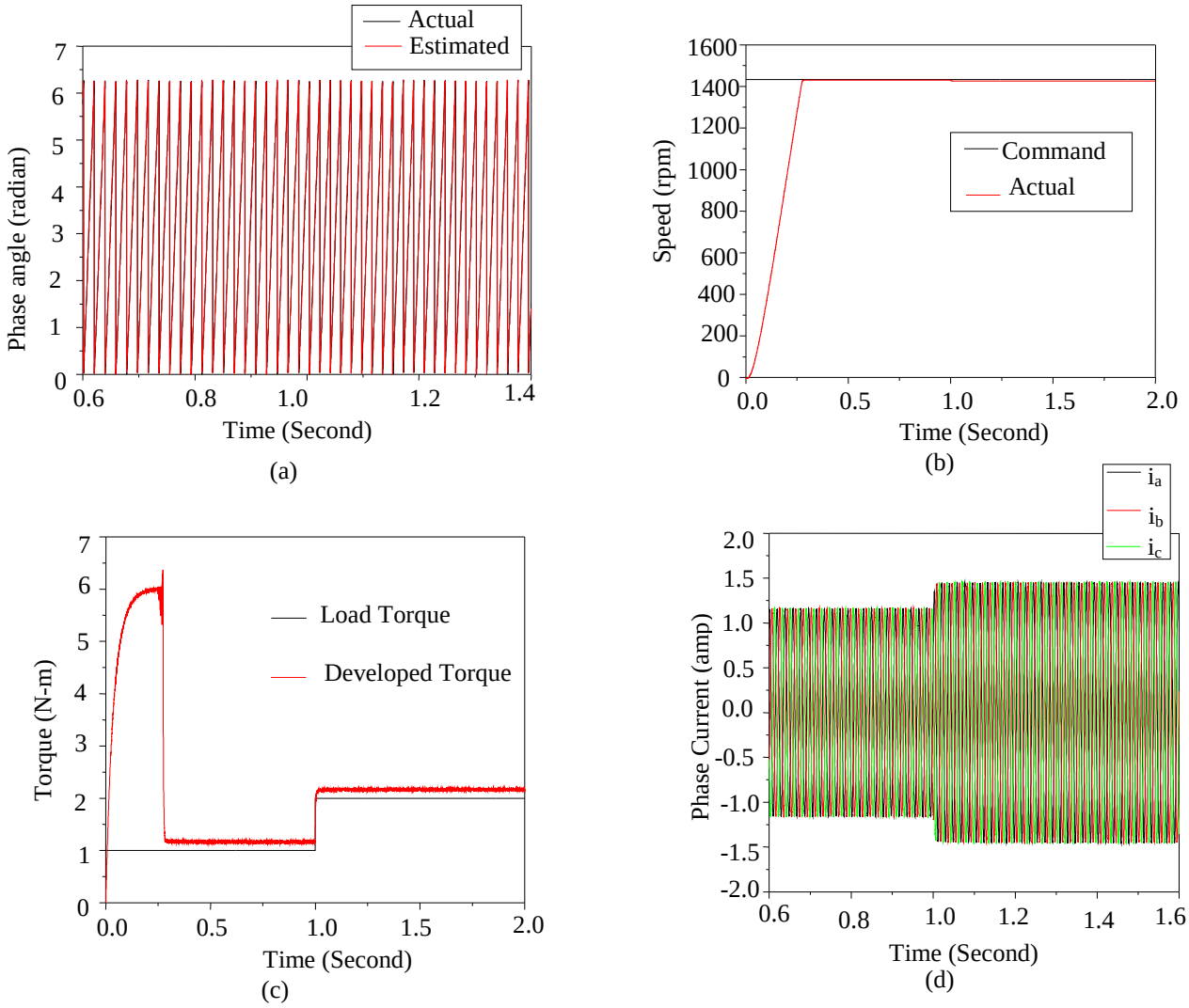

Figure 4.6 (a) Estimated rotor angle, (b) Speed, (c) Developed electromagnetic torque, and (d) Three phase currents for the proposed IM drive for change of load torque.

By applying 4S3P the motor was stared from standstill with load torque 1N.m. The estimated rotor angle and the speed responses for the change of load torque are given in Figs. 4.6(a) and (b). The speed response curve reached to the command speed at t=0.6sec. Sudden change of load torque does not affect the position estimation and causes a negligible oscillation in speed. Figs 4.6(c) and (d) show the corresponding torque and motor currents.

By using 4S3P, Sudden Change of Load Torque's speed response curve is taken same time.

4.4.2 Variation of Stator Parameters

To observe the effect of parameter variations, both the stator and rotor resistance were doubled (keeping other parameters constant) in 6S3P at t=0.8 second. Fig. 4.7(a) shows the effect of

stator resistance change on angle estimation. The estimated angle still follows the actual angle. Thus the change in resistance has negligible effect on the accuracy of rotor position estimation. Fig. 4.7(b) shows the effect of stator resistance change on speed response. The speed dose not drops at all due to change of stator resistance. The speed response curve reached to the command speed at t=0.32sec. Thus the drive performance is insensitive of stator parameter variation. Figs. 4.7(c) and (d) show that the developed torque and motor currents are also insensitive to stator parameter variation.

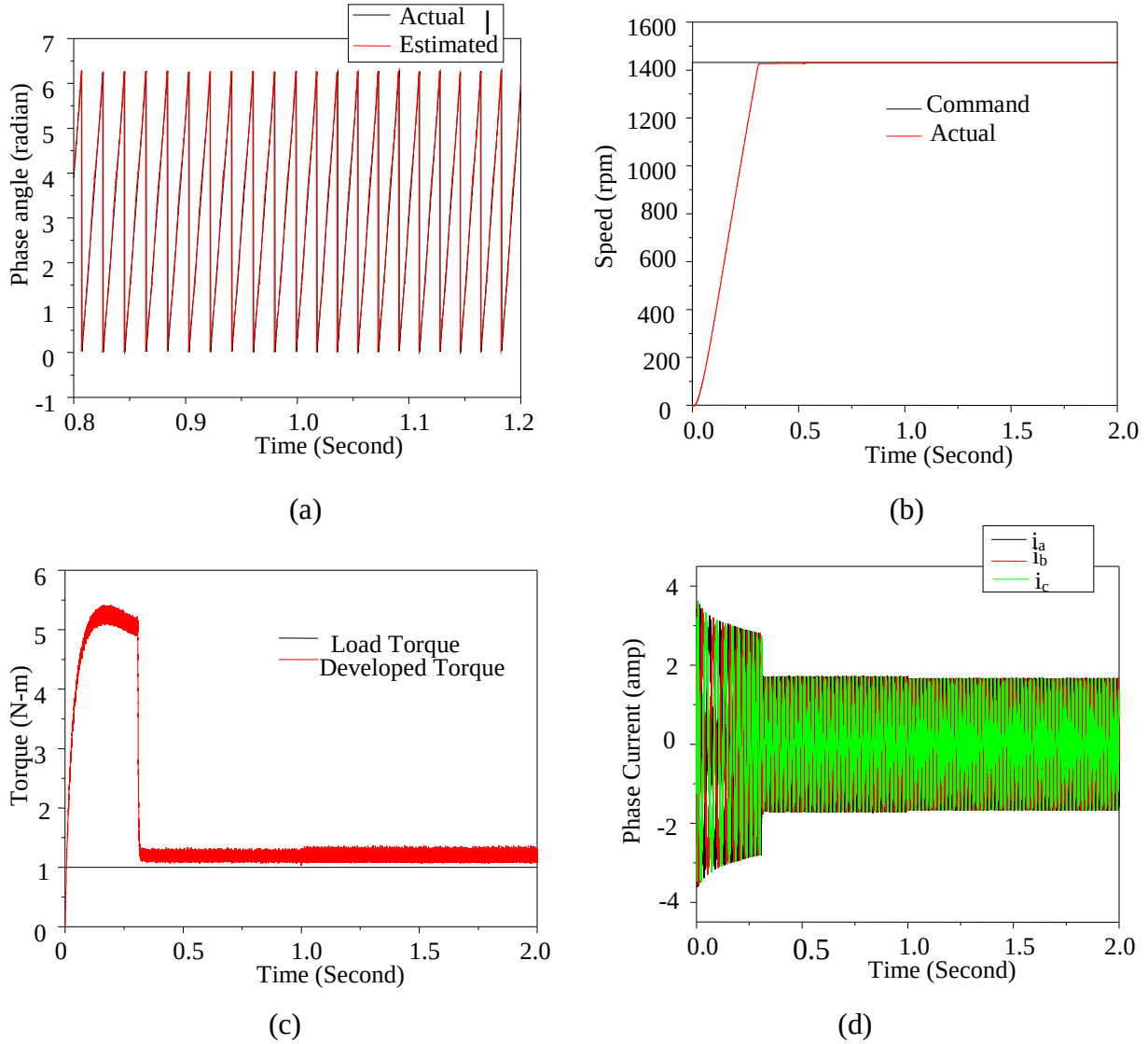

Figure 4.7 (a) Estimated rotor angle, (b) Speed, (c) Developed Electromagnetic torque, and (d) Three phase currents for the proposed IM drive for change of stator resistance.

By applying 4S3P,

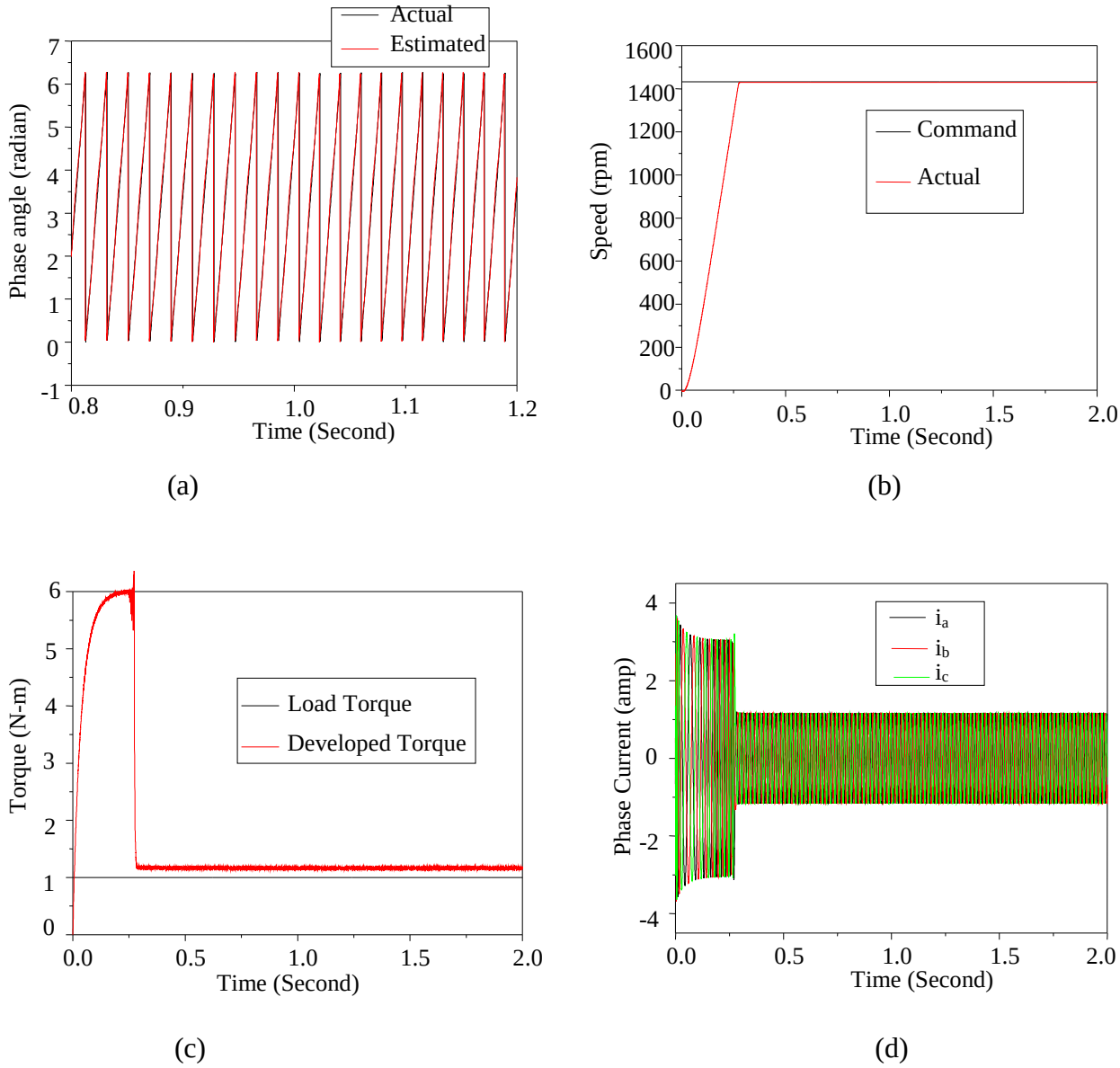

Figure 4.8 (a) Estimated rotor angle, (b) Speed, (c) Developed Electromagnetic torque, and (d) Three phase currents for the proposed IM drive for change of stator resistance by using PI.

Fig. 4.8(a) shows the effect of stator resistance change on angle estimation. The change in resistance has negligible effect on the accuracy of rotor position estimation. Fig. 4.8(b) shows the effect of stator resistance change on speed response. The speed dose not drops at all due to change of stator resistance. The speed response curve reached to the command speed at t=0.25sec. Figs. 4.8(c) and (d) show that the developed torque and motor currents are also insensitive to stator parameter variation.

By using PI controller, change of stator resistance's speed response response curve is taken same time.

4.4.3 Speed Reversal

Speed reversal is an essential requirement for high performance IM drives in 6S3P. Therefore, to monitor the effect of speed reversal, the command speed of the motor was reversal from 1500 rpm to -1500 rpm at t=1.0 second and again to 1500 rpm at t=2.0 second and repeated. Fig. 4.9(a) shows estimated rotor angle, When the motor runs at -1500 rpm, there is slight error between the estimated and actual angle but it is within the acceptable limit. The speed response for different set speeds is shown in Fig.4.9 (b). The speed response curve reached to the command speed at t=0.46sec. It is observed that the drive system follows both the forward and reverse direction reference track very quickly.

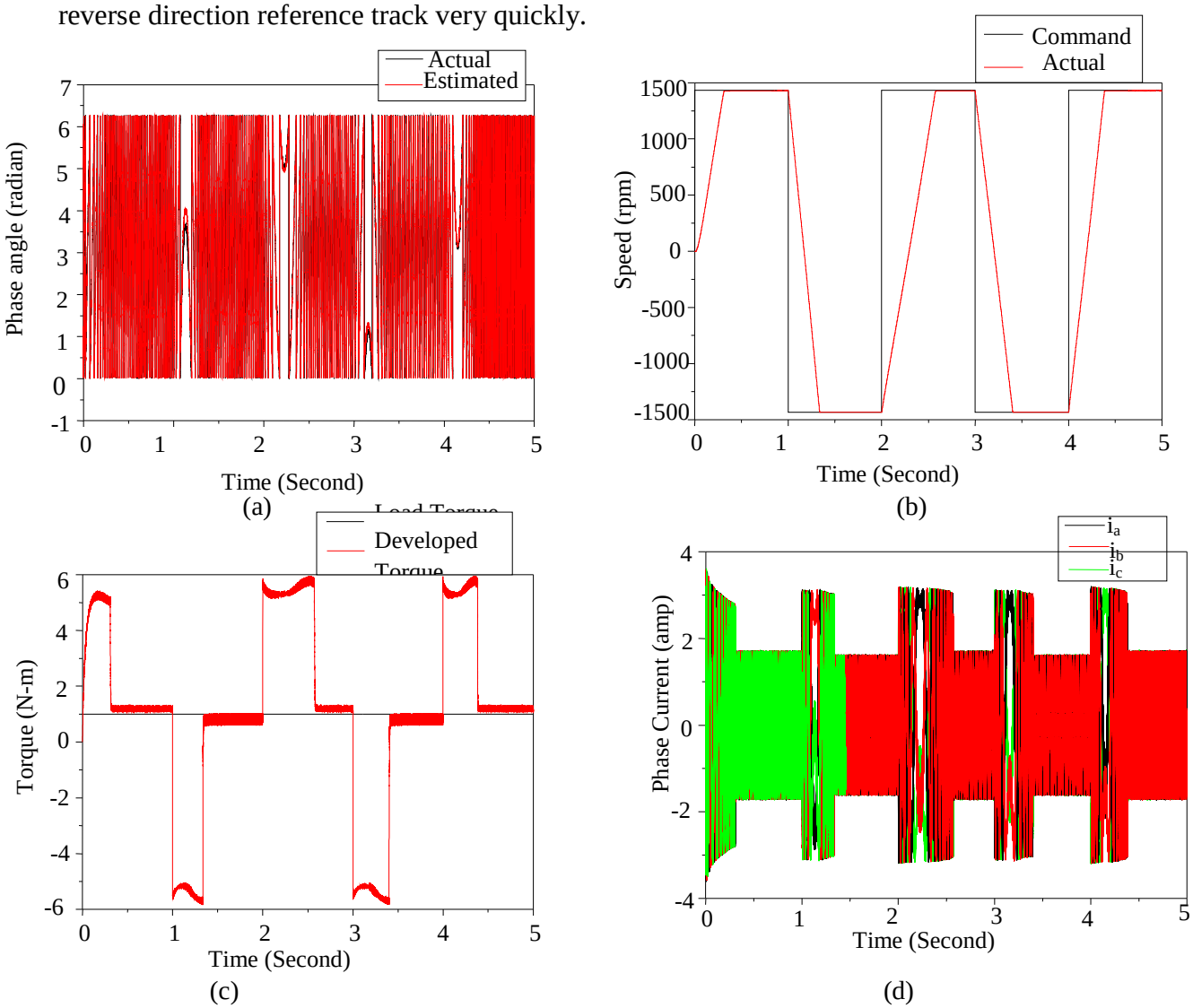

Figure 4.9 (a) Estimated rotor angle, (b) Speed, (c) Developed electromagnetic torque, and (d) Three phase currents for the proposed IM drive under speed reversal

The impact on developed electromagnetic torque and motor current due to speed reversal is shown in Fig. 4.9(c) and (d). The proposed control scheme produces less torque fluctuation at steady- state condition.

By applying 4S3P

Speed reversal is an essential requirement for high performance IM drives. Fig. 4.10(a) shows estimated rotor angle. The speed response for different set speeds is shown in Fig.4.10 (b). The speed response curve reached to the command speed at t=0.25sec. It is observed that the drive system follows both the forward and reverse direction reference track very quickly. The impact on developed electromagnetic torque and motor current due to speed reversal is shown in Fig..

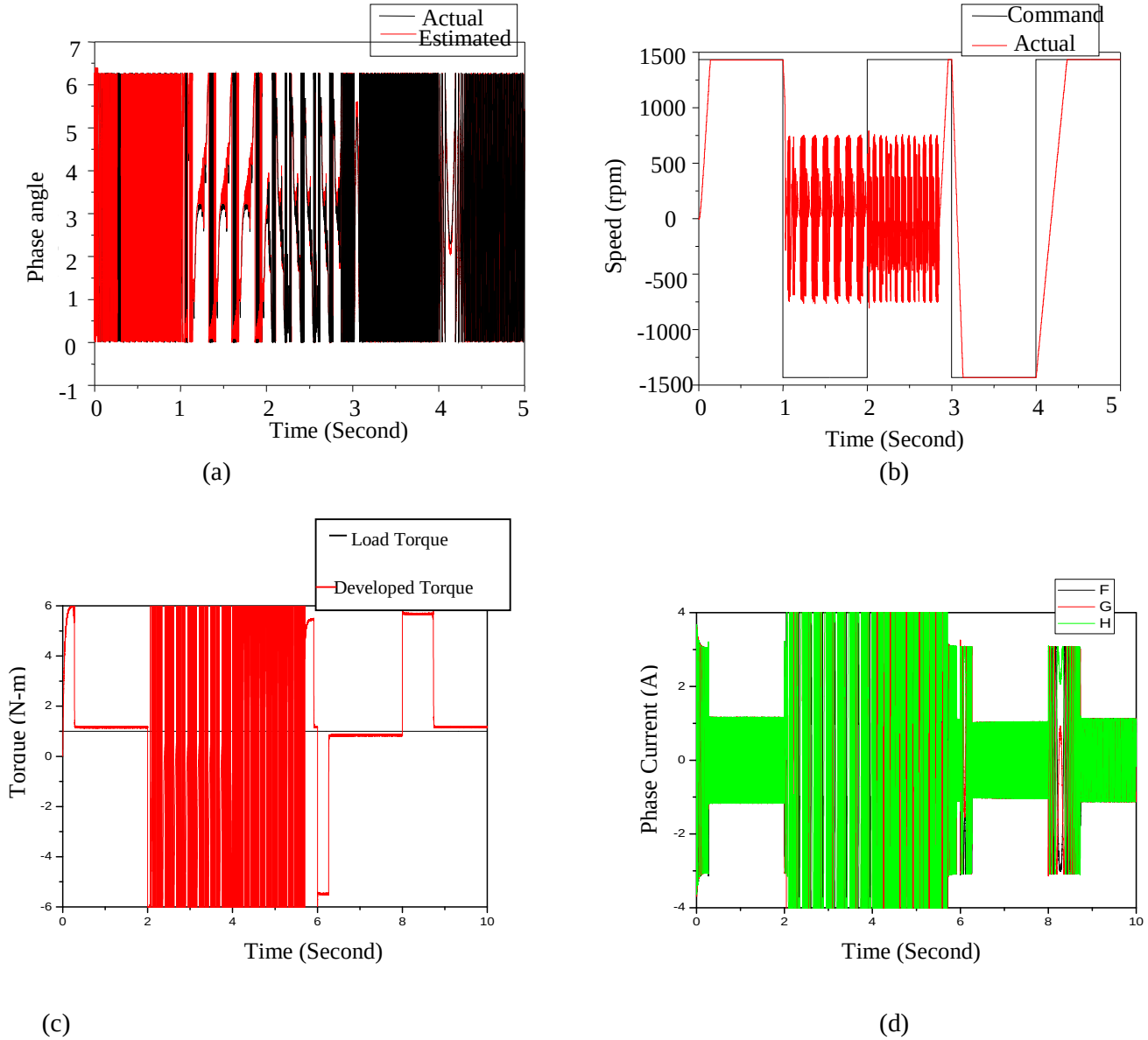

Figure 4.10 (a) Estimated rotor angle, (b) Speed, (c) Developed electromagnetic torque, and (d) Three phase currents for the proposed IM drive under speed reversal.

By using 4S3P, speed reversal's speed response curve is taken same time.

4.4.4 Ramp Speed Change

Like as speed reversal, ramp speed is also is an essential requirement for high performance IM drives in 6S3P. The controller set speed was gradually increased from zero and at time t=1.0 second it remained constant to 1500 rpm value. The estimated rotor position, speed response, developed electromagnetic torque and motor currents are shown in Fig. 4.11. The motor follows the command speed from the starting without any oscillation and steady- state error. The developed torque response is also similar to the starting performance.

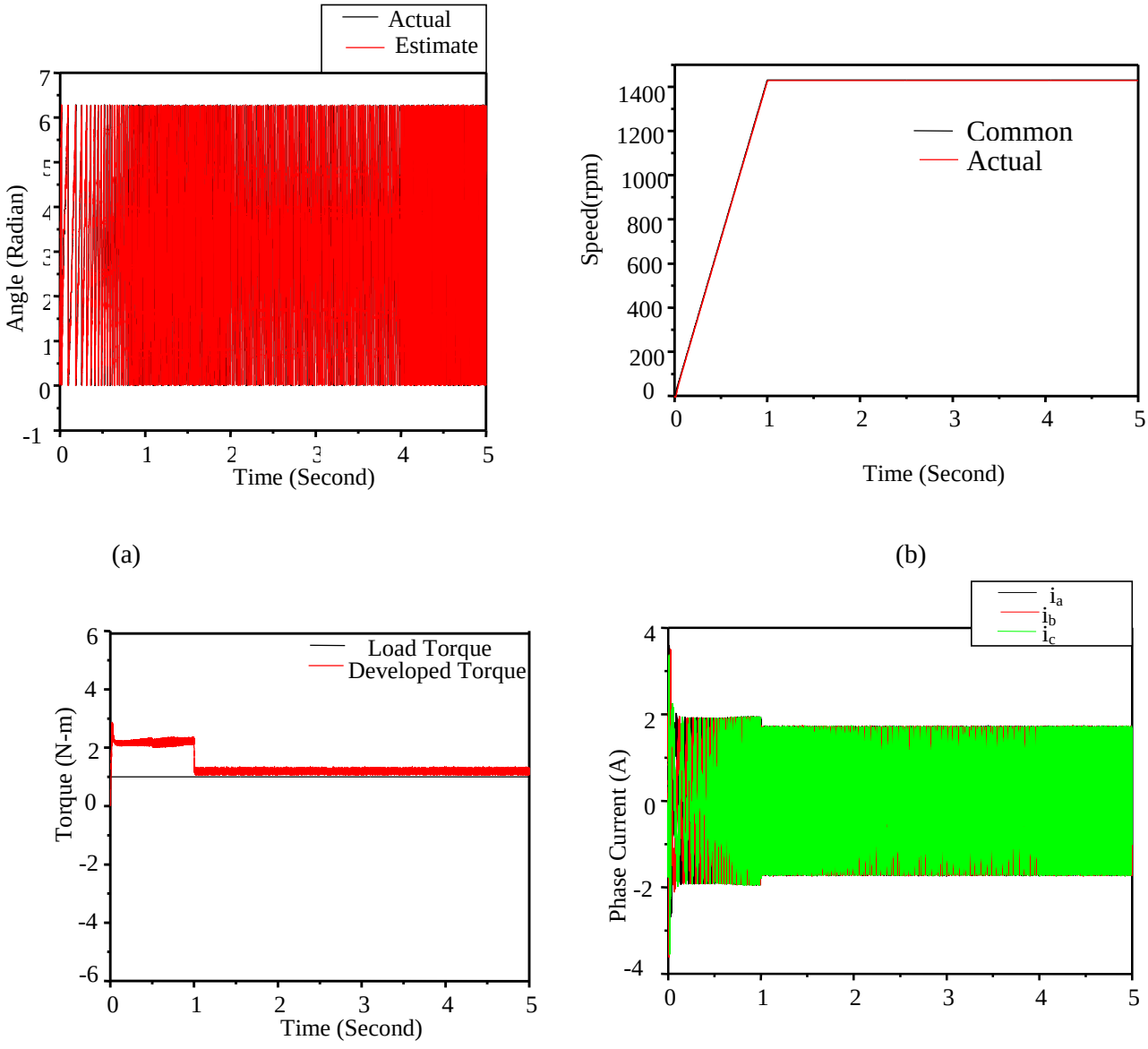

Figure 4.11 (a) Estimated rotor angle, (b) Speed, (c) Developed electromagnetic torque, and (d) Three phase currents for the proposed IM drive under Ramp Speed Chang

By using 4S3P,

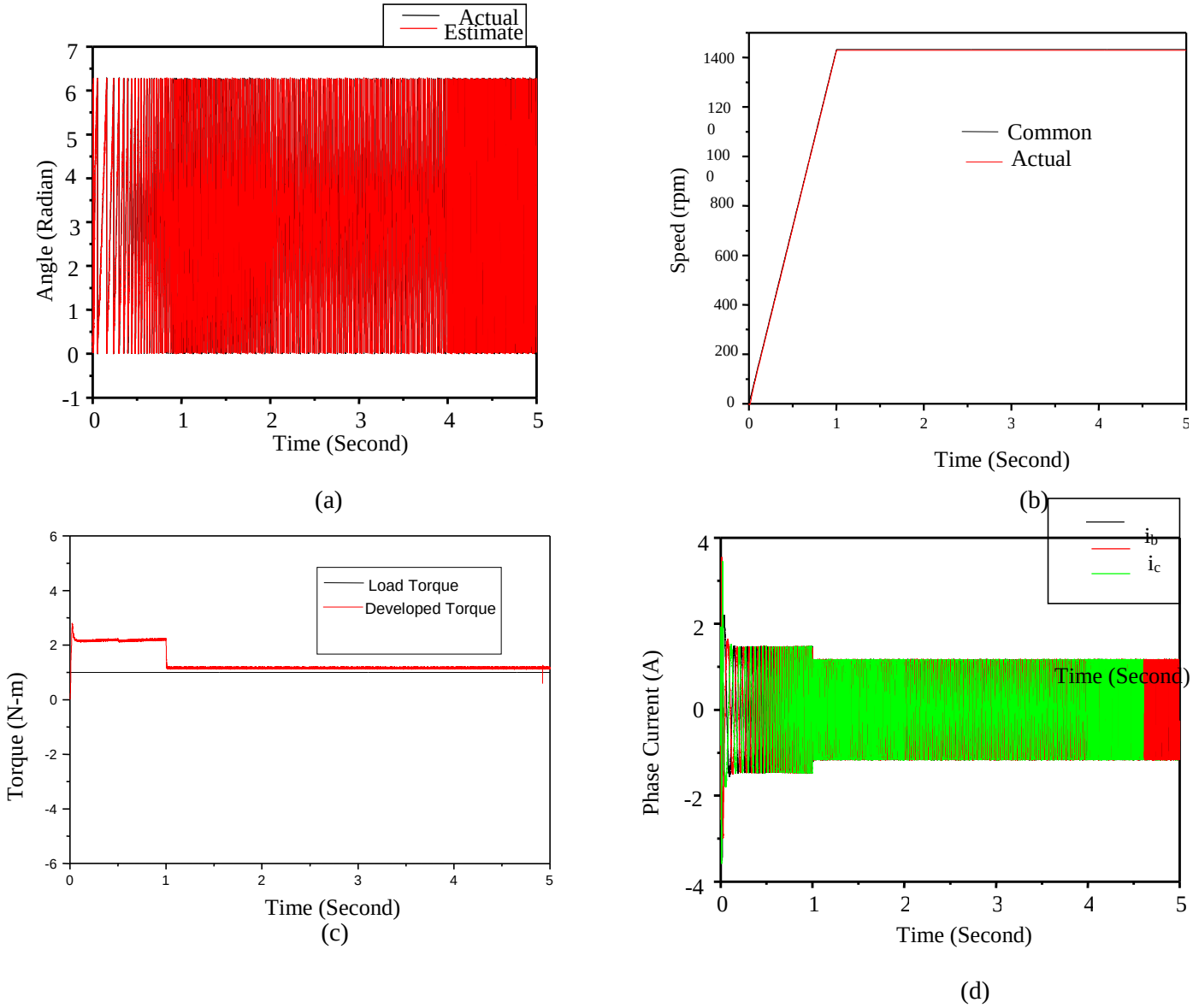

Figure 4.12 (a) Estimated rotor angle, (b) Speed, (c) Developed electromagnetic torque, and (d) Three phase currents for the proposed IM drive under Ramp Speed Change.

Ramp speed is also is an essential requirement for high performance IM drives. The controller set speed response curve was gradually increased from zero and at time t=1.0 second it remained constant to 1500 rpm value. The estimated rotor position, speed response, developed electromagnetic torque and motor currents are shown in Fig. 4.12. The motor follows the command speed from the starting without any oscillation and steady- state error.

By using 4S3P, Ramp Speed Change's speed response curve is taken same time.

4.4.5 Sudden Disturbance Torque

A sudden load disturbance (2.0 N.m) for a very short duration of 0.1 second was applied at 2=2.0 Sec. to the IM drive. Fig. 4.13(a) shows the actual and estimated rotor angle of the motor at that time period. The speed response of the IM is shown in Fig. 4.13(b). Simulation studies show that the proposed control scheme is still capable to estimate the rotor angle accurately. The speed response curve reached to the command speed at t=0.3 sec. Besides, the motor speed is insensitive to the sudden torque disturbance. Fig. 4.13(c) and (d) show the corresponding developed torque and motor currents.

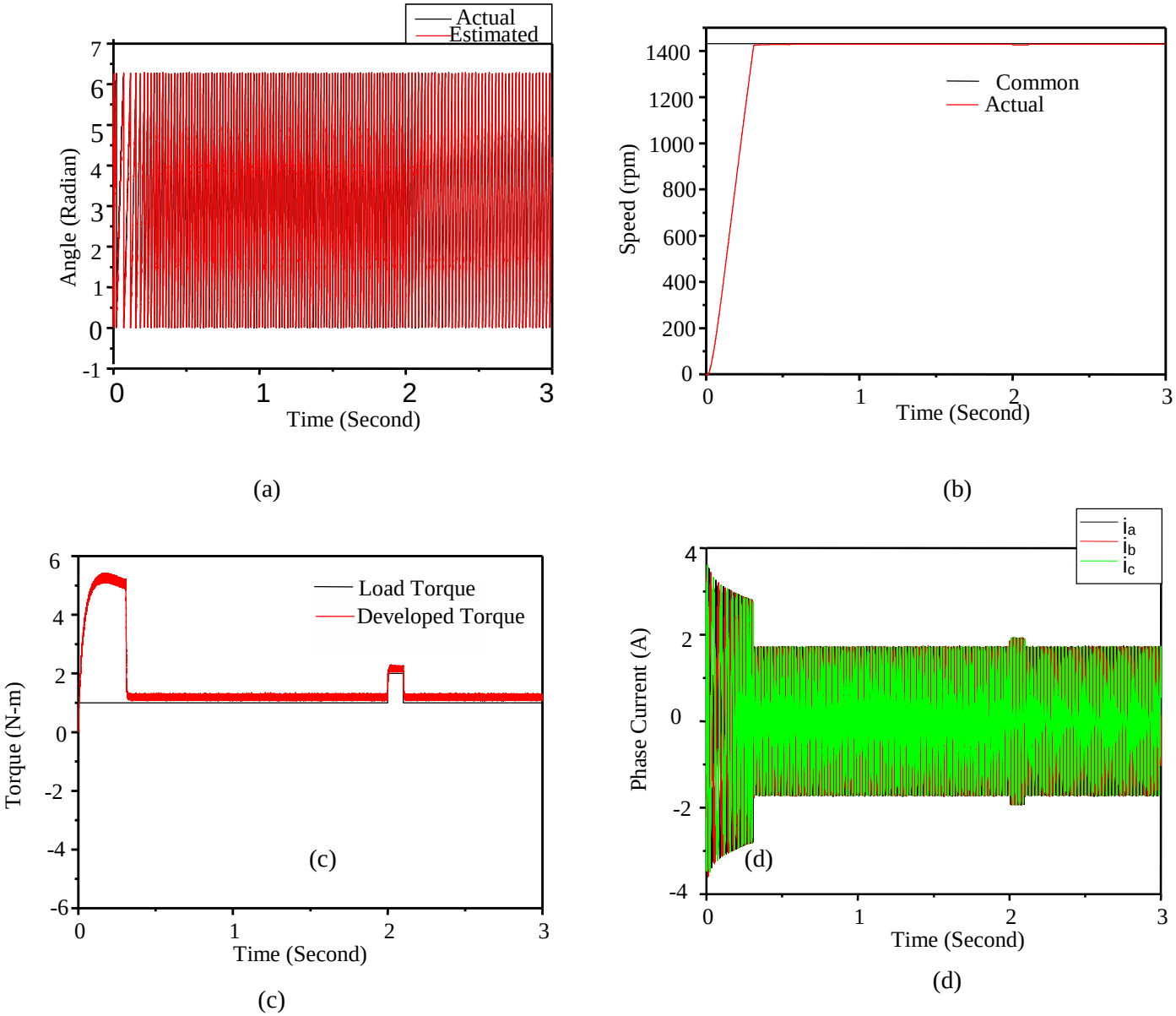

Figure 4.13 (a) Estimated rotor angle, (b) Speed, (c) Developed electromagnetic torque, and (d) Three phase currents for the proposed IM drive for sudden disturbance torque

By applying 4S3P,

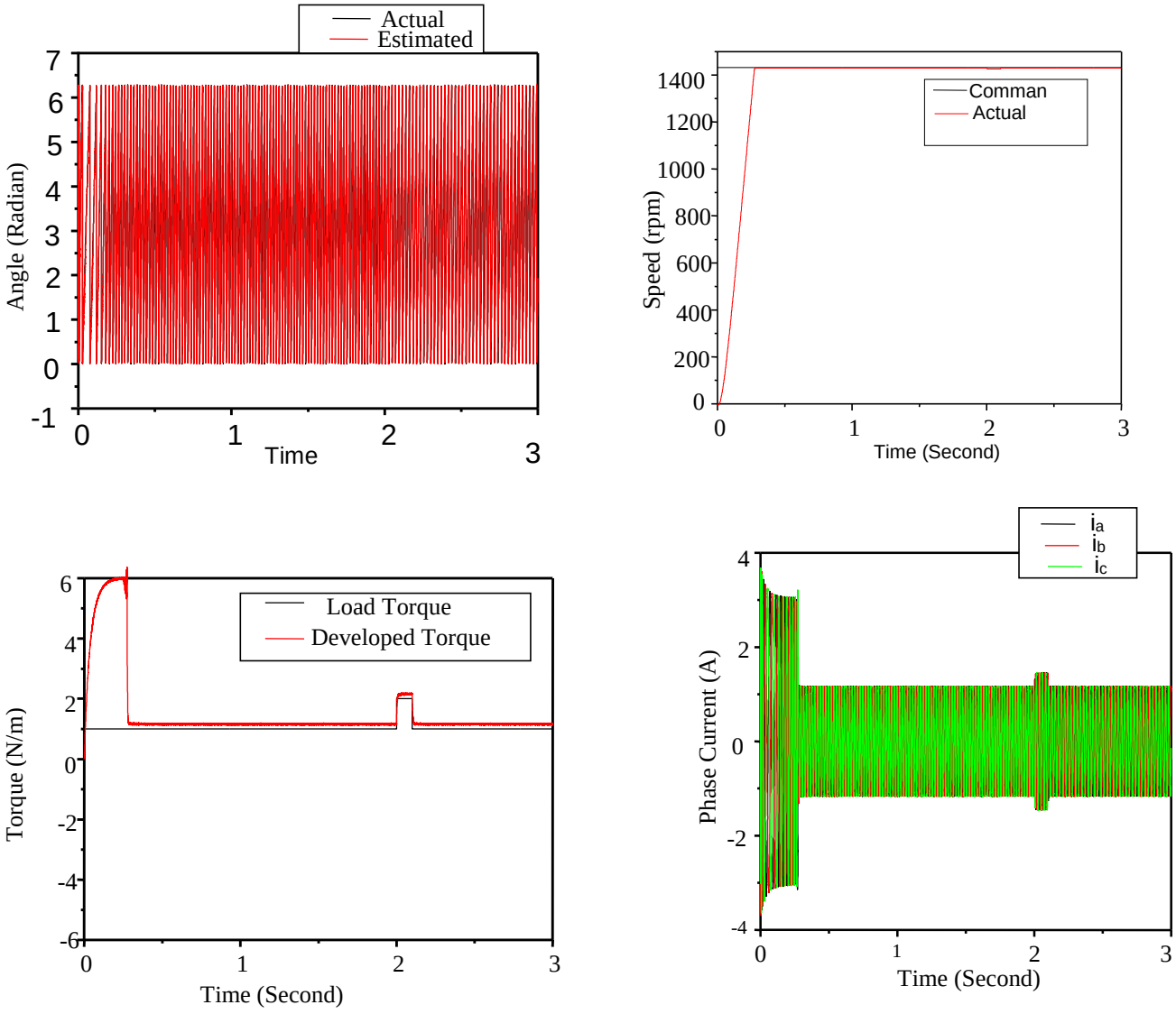

(c) (d)

Figure 4.14 (a) Estimated rotor angle, (b) Speed, (c) Developed electromagnetic torque, and (d) Three phase currents for the proposed IM drive for sudden disturbance torque.

A sudden load disturbance for a very short duration of 0.1 second was applied to the IM drive. Fig. 4.14(a) shows the actual and estimated rotor angle of the motor at that time period. The speed response of the IM is shown in Fig. 4.14(b). Simulation studies show that the proposed control scheme is still capable to estimate the rotor angle accurately. Besides, the motor speed is insensitive to the sudden torque disturbance. . The speed response curve reached to the command

speed at t=3.0sec. Fig. 4.14(c) and (d) show the corresponding developed torque and motor currents.

By using 4S3P, Sudden Disturbance Torque's speed response curve is taken same time.

4.5 Discussion

A direct torque control methodology for 4-switch 3-phase inverter fed induction motor drive is presented in this work. The control system needs very simple structure and is capable to estimate the torque and the stator flux acceptably. The results obtained and presented in this work indicate that the proposed control scheme produces very fast response of the IM drive without any overshoot and undershoot. The drive is also robust to load disturbances, and speed reversal conditions. Thus the proposed low cost control scheme is suitable for industry applications. The expected results of the proposed work are given below:

i. The 4S3P inverter based system replaces the 6S3P inverter based induction motor drive system.
ii. The torque and flux ripple is reduced.
iii. The harmonics in the current is reduced.
iv. The overall performance of the proposed 4S3P based control system is better than 6S3P inverter based control system.

4.6 Conclusion

The performance of the IM drive system in both transient and steady-state conditions will be improved with the use of 4S3P inverter and RTRNN based rotor position estimator. The drive system will be more reliable and cost effective. The speed response of the drive is expected to be better by using 4S3P than the previous IM drives. The drive will also be robust to load disturbances, parameter variations, and speed reversal conditions. The absence of position sensor and reduced inverter size will make the drive system more attractive for industry applications. The result observed very similar response of the IM drive by applying the 4S3P. The actual speed is very speedy to reach the command speed. Very fast response of the system without oscillation indicates the effectiveness of the proposed control scheme.

CHAPTER V

Conclusion

5.1 Discussion

This work presents a new technique to improve the performance of direct torque controlled VSI fed IM drive by using four switches in the inverter circuit. A mathematical model of the drive system was utilized to analyze the transient and steady-state responses of the motor. The performance of the induction motor drive under sudden change of load torque and speed reversal condition was also investigated in order to verify the robustness of the proposed control scheme. The proposed 4S3P inverter fed IM drive was found acceptable considering its cost reduction and other advantageous. The outline of the objectives of research work is given below:

i. To develop a control scheme for induction motor drive.

ii. To replace the 6S3P VSI-fed inverter with 4S3P VSI-fed inverter ensuring better performance of induction motor drive.

iii. To reduce the ripples in both of torque and flux than 6S3P based system.

iv. To make a comparison between the above two inverters on the basis of harmonics.

5.2 Conclusion

High performance control of Induction motor drive was done in the project. An effort was made to accommodate the robust and insensitive features of artificial neural network estimator. The total control law was designed on the consideration of field orientation control with magnetic saturation in Induction motor drive. Step by step development, analysis and study of the proposed methodology have been done in different chapters.

An optimal method to estimate the rotor position of the IM was the goal of this project. The estimated stator flux components are used to estimate the position of the rotor and provide accurate results under both transient and steady- state conditions. The RNN estimator is capable to estimate the stator fluxes and rotor angle at low motor speed. The estimator is also accurate and robust to perturbation of parameters.

The work was presented in this dissertation used artificial neural network based flux estimation and suitable control law for high performance control of Induction motor drive. For these purposes mathematical models of the three phase Induction motor are written in d-q reference frame under different operating conditions.

The artificial neural network based rotor flux estimator presented in this dissertation has been shown is very accurate and robust to parameter changes. It uses evolutionary algorithm learning based correlated α- and β- axes flux estimation and found to work satisfactorily under transient and steady- state conditions. Estimated flux components utilized to estimate the positions of the rotor flux axis also produce accurate results under steady state and transient conditions.

The proposed control methodology originates from the speed and torque error processing through controllers instead of instantaneous switching. A direct torque control methodology for 4-switch 3-phase inverter fed induction motor drive presented in this work. The control system needs very simple structure and is capable to estimate the torque and the stator flux acceptablyThe proposed method generates the required voltage components which were used to find out the required voltage magnitude and its position from the inverter. The results of the proposed control system were compared with the control system having PI controller. Very fast speed response, less torque pulsations and capable to work under different operating conditions indicate the efficacy of the proposed control method. It has been observed that the proposed control method was robust against parameter changes and disturbances. Based on the results from the previous chapters and the above discussion it can be concluded that the proposed control scheme provides high performance control for Induction motor drives.

The performance of the IM drive was also investigated for different operating conditions. The proposed control scheme provides good speeds response of the motor when the load torque fluctuates from its initial value. The IM drive follows the reference track very quickly during speed reversal and ramp change of speed. The system was also found robust against computational errors present in the physical system.

Based on the results from previous chapters and the above discussion it can be conclude that the proposed CRTRL based 4S3P control scheme was suitable for present industry applications.

5.3 Proposed for Future Research

The research work presented in this dissertation provides a methodology to utilize the ANN for position sensor less operation of IM drive. The proposed system may be implemented in practical environment and compares the practical results with those obtained from this study. It is suggested that this work can be tested for an IM in order to verify the effectiveness of the proposed control methodology.

To produce required variable dynamics from the drive system PI controller constants may be obtained using online tuning through genetic algorithms. Further, the researchers may work with fuzzy- neuron estimators instead of RNN estimators. Newly, introduced training methods, such as practical swarm optimization technique may be tested for training the estimators. These flux and position estimators are expected to work effectively under all operating conditions.

References

[1] C. M. Liaw, Y. S. Kung, and C. M. Wa, “Design and implementation of a high performance field-oriented induction motor drive,” IEEE Trans. Ind. Electron, Vol. 38, no. 4, pp. 275-282, Aug. 1991.

[2] G. R. Slemon, “Electric Machine and Drives,” Addisio-Wesly, Reading, MA, 1992.

[3] S. B. dewan, G.R. Slemon, and A Straughen, “Power Semiconductor Drives,” willy Interscience, New York, 1984.

[4] K. B. Nordin, D. W. Novtny, and D. S. Zinger, “The influence of motor parameter deviation in feedforward field orientation drive system,” IEEE-IAS Trans, vol IA-21, no. 4, pp 1009-1015, July/August 1985.

[5] R. D. Lorenz, and D. W. Novonty, “ Optimal utilization of induction machines in field oriented drives,” J. Electrical and Electric Engine, Australia,Vol. 10, no. 2, pp. 95-100, June 1990.

[6] S Saravanasundaram and K.Thanushkodi, 2008. “Compound Active Clamping Boost Converter-Three Phase Four Switch Inverter Fed Induction Motor.” International Journal olCoi’nputer Science and Network Security. Vol. 8. No. 8. pp. 358-361.

[7] M N Uddin. T. S. Radwan, and M. A. Rahman. 2006, “Performance Analysis of a Cost Effective 4-Switch, 3-Phase Inverter Fed IM Drive.” Iranian Journal of Electrical and Computer Engineering. Vol. 5. No. 2. Pp. 97-102

[8] M N. Uddin. T. S. Radvan. and M. A. Rabman, 2004. “A Cost Effective 4-Switch. 3-Phase Inverter Fed PM Motor Drive.” Proceedings of International Conference on Electrical & Computer Engineering. pp. 339-342. Dhaka, Bangladesh.

[9] M N Uddin. T S. Radwan. and M. A Rahman, 2006, “Fuzzy-logic-controller-based cost efl’ecti e four-switch three-phase inverter-fed 1PM synchronous motor drive system.” IEEE Trans on Industry Applications. Vol. 42. No. 1, pp. 21-30.

[10] Phan Quoc Dtung. Le Minh Phuorw. Tran Cong Binh. and Nguyen Minh Hoang. 2007. ‘A Complete Implementation of Vector Control for a Four-Switch Three-Phase ln\crler Fed IM Drie.” International Symposium on Electrical & Electronics Enwneering. HCM City. Vietnam.

[11] J.M. Zurada, Introduction to Artificial Neural Sustem, St. Poui, MN: Wes, 1992.

[12] Junwei Ge, Jing Sha, and Yiqiu Fang, “ A New Back Propagation Algorithm with Chaotic Learning Rate”, Proceedings of IEEE International Conference on Software Engineering and Science (ICSESS), pp.404-407, 16-18 July, 2010, Beijing, China.

[13] M. Islam, M. R. Rana, S.U. Ahmed, A.N.M Enamul Kabir, and M. Shahjahan, "Training Neural Network with Chaotic Learning Rate", Proceedings of International Conference on Emerging Trends in Electrical and computer Technology (ICETECT), pp. 781-785, 23-24 March 2011, Tamil Nadu, India.

[14] B.K. Bose, "Expert System fuzzy, logic and neural network application in power electronics and motion control," Proc. IEEE, vol. 82, no, 8, pp. 1303-1323, Aug. 1994.

[15] L.E.B. Da Silva, B. K. Bose, and J.O.P Pinto, "Recurrent-neural-network based implementation of a programmable cascaded low-pass filter used in stator flux synthesis of vector- controlled induction motor drive", IEEE Transactions on Industrial Electronics, Vol. 46, issue 3, pp. 662-665, June-1999.

[16] Md. Abdur Rafiq, Naruttam Kumar Roy, and B.C. Ghosh, "An Improved Induction Motor Rotor Flux Estimator Based on Correlated Real Time Recurrent Learning Algorthm", Proceedings of the International Conference on Power System Analysis, Visakhapatnam, AP, India, pp. 866-873,2008.

[17] Cui Wei, K.T. Chau, Wang Zheng, and J.Z. Jiang, "Application of Chaotic Modulation to Ac Motors for Harmonic Suppression", Proc. of IEEE International Conference on Industrial Technology (ICT)", pp. 2343-2347, 15-17 Dec. 2006, Mumbai, India.

[18] D.C. Huynch, M.W. Dunnigan, and S.J. Finney, "Vector Controlled Induction Motor Drives Based on Chaotic SVPWM", Transactions of China Electro technical Society, 2009-2011.

[19] D.C. Huynch, M.W. Dunnigan, and S.J. Finney, "Energy efficient control of an induction machine using a chaos particle swarm optimization algorithm", Proc. of IEEE International Conference on power and Energy (PECon), pp. 450-455, Nov. 29 2010-Dec, 1 2010, Kuala Lumpur, Malaysia.

[20] Bambang Purwahyudi, Soebagio, and M. Ashari, "RNN Based Rotor Flux and speed Estimation of Induction Motor", International Journal of Power Electronics and Drive System (IJPEDS), vol. 1, no.1, pp.58-64, September 2011.

[21] A Derdiyok, "Speed sensorless control of induction motor using a continuous control approach of sliding-mode and flux observer," IEEE Trans. Ind. Electron, Vol. 52, No.4, 2000, pp. 1170-1176.

[22] C Lascu, I Boldea and F Blaabjerg, "Direct torque control of Sensorless induction motor drives : A sliding mode approach," IEEE Trans. Ind. Applicat, vol. 40, No.2, 2004, pp. 582-590.

[23] C Lascu, I Boldea and F Blaabjerg, " Very-low-speed variable-structure control of sensorless induction machine drives without signal injection," IEEE Trans. Ind. Applicat., Vol. 41, No, 2, 2005, pp. 591-598.

[24] P Vaclavek and P Blaha, “Lyapunov-function-based flux and speed observer for AC induction motor sensorless control and parameter estimation,” IEEE Trans. Ind. Electron, vol. 53, no. 1,2006, pp. 138-145.

[25] MJ Duran, JL Duran F Perez and J Fermandez, “Induction-motor sensorless vector control with in-line parameter estimated and over-current protection,” IEEE Trans Ind. Electron, vol. 53, no.1, 2006, pp-154-161

[26] Paul C.Crause,Oleq Wasynezuk & Scott D,Sudhoff,1995,”Analysis of electrical machines”,Institute of electrical & electronics engineer.

[27] I.Boldea,S.A.Nassar,1999,”Electria drives”, CRC press LLC.

[28] Leonard,W,1996, “ Control of Electrical Drives”, Springer- Verlag, Berlin, Heidelberg.

[29] Luis romeral, Antoni Arias, Emiliano Aldabas, and Marcel, G. Janye, “Novel direct torque control (DTC) scheme with fuzzy adaptive torque-ripple reduction “, IEEE Transaction on Industrial Electronics, June, Vol. 50, no. 3, pp. 487-492,2003.

[30] Vas, P. “ Vector Control of AC Machines”, Oxford University Press, Oxford,1993.

[31] M N Uddin. T S. Radwan. and M. A Rahman, “Fuzzy-logic-controller-based cost efl’ecti e four-switch three-phase inverter-fed 1PM synchronous motor drive system.” IEEE Trans on Industry Applications. Vol. 42. No. 1, pp. 21-30,2006.

[32] Ivonne,Y.B.Sun,D,and He,Y.K(2008),Study on Inverter Fault-Tolerant Operation of PMSM DTC,Journal of Zhejiand University Science A,9(2), ,pp,156-164 .

[33] Simon Haykin. 2001. “Neural Networks a Comprehensie Foundation.” 2’ edition. Pearson education. Inc.

[34] Maurizio Cirrincione. Marcello Pucci, Giansalvo Cirrincione, and Gerard-Andre Capolino. 2004. “A New Adaptive Integration Methodology for Estimation Flux in Induction Machine Drives.” IEEE Transactions on Power Electronics. Vol.19. No.1. pp 25-33.

[35] B Widrow and S D Steam. 1985. Adaptive Signal Processing.' Englevood Cliffs. NJ Prenuce-Hall

[36] S Bologani. G. S. Buja. 985. Control System Design of a Current Inverter Induction Motor Drives.' IEEE Trans. on Industry Applications. Vol IA-21. No 5. pp 1145-1153.

APPENDIX

APPENDIX- A

IPMSM Parameters

Number of phases = 3
Number of poles = 4
Rated frequency = 60 Hz
Rated power = 1 hp
Rated input line to h e voltage= 208 V
q-axis inductance L_q = 0.07957 H
d-axis inductance L_d = 0.04244 H
Stator resistance per phase r_s = 1.93 Ω
Inertia constant J_m = 0.003 Kg.m^2
Rotor damping constant B_m= 0.0008 (N-m)/rad./sec.
Permanent magnet flux linkage ψ_m = 0.3 14 volt/rad./sec.
Magnet type = Samarium Cobalt.

Speed loop: Kp = 0.04, Ki = 10.0

Weights of the RNN: W_1 =W_2 = 0.1, W_1 =W_2 = 0.0001, W_1 =W_2 = 0.068, W_1 =W_2 = −0.05, W_1 =W_2 = 0.0001.